AD_____

Award Number: W81XWH-09-1-0475

TITLE: Deregulated miRNA in Mammary Epithelium by Tumor Promoting Extracellular Matrix

PRINCIPAL INVESTIGATOR: Bin Shan, M.D., Ph.D.

CONTRACTING ORGANIZATION: Tulane University Health Sciences Center
New Orleans, Louisiana 70112

REPORT DATE: August 2010

TYPE OF REPORT: Final

PREPARED FOR: U.S. Army Medical Research and Materiel Command
Fort Detrick, Maryland 21702-5012

REPORT DOCUMENTATION PAGE

Form Approved
OMB No. 0704-0188

1. REPORT DATE	2. REPORT TYPE	3. DATES COVERED
August 2010	Final	1 August 2009 – 31 July 2010

4. TITLE AND SUBTITLE

Deregulated miRNA in Mammary Epithelium by Tumor Promoting Extracellular Matrix

5a. CONTRACT NUMBER

5b. GRANT NUMBER
W81XWH-09-1-0475

5c. PROGRAM ELEMENT NUMBER

6. AUTHOR(S)

Bin Shan

E-Mail: bshan@tulane.edu

5d. PROJECT NUMBER

5e. TASK NUMBER

5f. WORK UNIT NUMBER

7. PERFORMING ORGANIZATION NAME(S) AND ADDRESS(ES)

Tulane University Health Sciences Center
New Orleans, Louisiana 70112

8. PERFORMING ORGANIZATION REPORT NUMBER

9. SPONSORING / MONITORING AGENCY NAME(S) AND ADDRESS(ES)
U.S. Army Medical Research and Materiel Command
Fort Detrick, Maryland 21702-5012

10. SPONSOR/MONITOR'S ACRONYM(S)

11. SPONSOR/MONITOR'S REPORT NUMBER(S)

12. DISTRIBUTION / AVAILABILITY STATEMENT
Approved for Public Release; Distribution Unlimited

13. SUPPLEMENTARY NOTES

14. ABSTRACT
The goal of this project is to identify the miRNAs that are altered by the aberrant extracellular matrix within the tumor microenvironment, particularly the fibrillary collagen, Collagen type I (Col-1). The biochemical and biophysical properties of the extracellular matrix (ECM) are essential to the establishment and maintenance of epithelial polarity. Increased ECM rigidity caused by deposition of fibrillar collagen, e.g., type I collagen (Col-1), promotes loss of epithelial polarity and tumor progression. microRNAs are small non-coding RNAs that regulate gene expression and fundamental cellular processes. The current study explores a link between microRNAs and Col-1 deposition using organotypic three-dimensional culture in which epithelial cells are embedded within Matrigel, a mimic of basement membrane matrix (rBM 3-D). rBM 3-D culture of MCF-7 gave rise to acini that consisted of a polarized monolayer of epithelial cells facing a central lumen, an in vitro phenomenon of epithelial polarity. Supplementation of Col-1 disrupted acini and up-regulated the expression of miR-21, a well-documented oncogenic microRNA, via a post-transcriptional mechanism, which correlates with a decrease in two miR-21 targets, programmed cell death 4 and phosphatase and tensin homologue. In summary, our findings provide a link between altered ECM composition/rigidity and the expression of oncogenic microRNAs. The current study also suggests a novel post-transcriptional mechanism for regulation of miR-21 expression at maturation from pre-miR-21 to mature miR-21. We also compared the expression of miRNAs in rBM 3-D and 2-D cultures of the non-invasive MCF-7 and the invasive MDA-MB231 cells. Our findings revealed a profound difference in miRNA profiles between 2-D and rBM 3-D cultures within each cell type. The disparate miRNA profiles correlated with distinct mass morphogenesis of MCF-7 and invasive stellate morphogenesis of MDA-MB231 cells in rBM 3-D culture. Supplementation of the tumor promoting type I collagen in rBM 3-D culture substantially altered the miRNA signature of mass morphologenesis of MCF-7 cells in rBM 3-D culture. Lastly, overexpression of the differentially expressed miR-200 family member miR429 in MDA-MB231 cells attenuated their invasive stellate morphogenesis in rBM 3-D culture. In summary, we provide the first miRNA signatures of morphogenesis of human breast cancer cells in rBM 3-D culture and warrant further utilization of rBM 3-D culture in investigation of miRNAs in breast cancer.

15. SUBJECT TERMS
microRNA, extracellular matrix, breast cancer.

16. SECURITY CLASSIFICATION OF:			17. LIMITATION OF ABSTRACT	18. NUMBER OF PAGES	19a. NAME OF RESPONSIBLE PERSON
a. REPORT	b. ABSTRACT	c. THIS PAGE			USAMRMC
U	U	U	UU	36	19b. TELEPHONE NUMBER *(include area code)*

Table of Contents

INTRODUCTION

The integrity of the basement membrane (BM) is essential for homeostasis of normal mammary epithelium (1). Disruption of the BM by deposition of fibrillar collagen has been associated with initiation and progression of breast cancer in patients and experimental models (3). miRNAs are small non-coding RNAs that down-regulate translation of a target mRNA by partial complementarity with its target sequences within the 3' untranslated regions. Profiling miRNA in human breast samples and breast cancer cell lines reveals deregulated expression of a number of miRNAs, such as up-regulated miR-21 and miR-10b, and down-regulated miR-125a and miR-200c (2). This proposal hypothesizes that deregulated expression of miRNAs contributes to resistance of breast cancer cells to differentiation promoting ECM, whereas miRNAs modulated by the tumor promoting ECM contribute to aggressiveness of breast cancer cells. *Aim 1*–To identify miRNAs that are differentially expressed in monolayer 2-D culture and the reconstituted BM Matrigel based three-dimensional culture (rBM 3-D) between MCF-7 (tumorigenic/non-metastatic) and MDA-MB-231 (tumorigenic/metastatic) cells. *Aim 2*–To identify miRNAs whose expression is modulated by the tumor promoting ECM and which correlate with disruption of mammary gland acini and invasive growth. The prototype of the tumor promoting ECM is generated by supplementing rBM with type I collagen (rBM+Col-1). miRNA profiles will be compared between rBM 3-D and rBM+Col-1 3D cultures in MCF-7 cells. The rBM-Col-1 responsive miRNAs will be identified. Disruption of mammary gland acini and invasive growth will be assessed relative to an altered miRNA response to rBM+Col-1.

BODY

1. To establish lrECM 3D (rBM 3-D) cultures of MCF-10A, MCF-7, and MDA-MB231 cells using Matrigel. (as stated in Aim 1).

> We successfully established rBM 3-D culture of MCF-7 and MDA-MB231 cells. We encountered technical barriers in culturing MCF-10A cells in rBM 3-D culture and decided to drop the cell line because it is not essential to our overall hypothesis and objective.

2. To carry out TaqMan miRNA arrays on RNA samples collected from MCF-10A, MCF-7, and MDAMB231 cells in lrECM 3D cultures. To identify the miRNAs that respond to lrECM by comparing the miRNA profiles between plastic 2D monolayer culture and lrECM of in MCF-10A. Within the panel of the lrECM responsive miRNAs, focus is to identify the miRNAs whose response to lrECM is greater than 2-fold and in MCF-10A cells and absent in MCF-7 and MDA-MB231. To correlate the absent miRNA response with reduced formation of mammary gland acinus in MCF-7 and MDA-MB231 when compared with MCF-10A. (as stated in Aim 1)

> We profiled miRNA expression in 2-D and rBM 3-D cultures of MCF-7 and MDA-MB231 cells. We used miRNA arrays provided by LC Sciences instead of RT-PCR because miRNA arrays are more cost-effective. We identified dozens of miRNAs that correlated with distinct morphogenesis of MCF-7 and MDA-MB231 cells in rBM 3-D. These miRNAs included several well-documented tumor-modulating miRNAs, such as the members of miR-200 family. A detailed description and discussion of the results were presented in a submitted manuscript (see Appendix B).

3. To determine the function of the lrECM responsive miRNAs in formation of mammary gland acinus. The functional assays, assessment of mammary gland acini, will be restricted to the miRNAs whose response to lrECM, including both down-regulation and up-regulation, is greater than 2-fold and present in MCF-10A but absent in MCF-7 and MDA-MB231. The selected

miRNA response will be compromised in MCF-10A cells and restored in MCF-7 and MDA-MB231 cells followed by assessment for formation of mammary gland acini. (as stated in Aim 1)

For functional analysis, we focused on miR-429, a miRNA-200 family member that exhibited higher expression in MCF-7 than MDA-MB231 in rBM 3-D culture. Overexpression of miR-429 in MDA-MB231 cells repressed the expression of ZEB1, increased the expression E-cadherin, and induced a transition from the invasive stellate morphology to the non-invasive mass morphology. A detailed description and discussion of the results were presented in a submitted manuscript (see Appendix B).

4. To establish lrECM-Col 3D cultures of MCF-10A, MCF-7, and MDA-MB231 cells using Matrigel supplemented with type I collagen. (as stated in Aim 2)

We establish rBM 3-D culture of MCF-7 and MDA-MB231 cells in the presence or absence of Col-1. We focused our miRNA profiling on MCF-7 cells in rBM 3-D culture +/- Col-1 because MCF-7 exhibited a greater distortion of morphogenesis in response to Col-1.

5. To carry out TaqMan miRNA arrays on RNA samples collected from MCF-10A, MCF-7, and MDAMB231 cells in lrECM and lrECM-Col 3D cultures. To identify the miRNAs that respond to lrECM-Col by comparing the miRNA profiles between lrECM and lrECM-Col 3D cultures in MCF-10A, MCF-7 and MDA-MB231. Within the panel of the lrECM-Col responsive miRNAs, focus is to identify the miRNAs consistently respond to lrECM-Col greater than 2-fold in all three cell lines. (as stated in Aim 2)

We profiled the expression of miRNAs in rBM 3-D culture +/- Col-1 and identified dozens of miRNAs that were dysregulated by Col-1. A detailed description and discussion of the results were presented in a published manuscript and a submitted manuscript (see Appendix A & B).

6. To determine the function of the lrECM-Col responsive miRNAs in formation of mammary gland acinus. The functional assays, assessment of mammary gland acini, will be restricted to the miRNAs whose response to lrECM-Col, including both down-regulation and up-regulation, is present in all three cell lines. The selected miRNA response will be compromised in MCF-10A, MCF-7 and MDA-MB231 cells followed by assessment for disruption of mammary gland acini and invasive growth. (as stated in Aim 2)

We attempted over-expression of miR-21 in MCF-7 cells. However, maturation of miR-21 is a rate-limiting factor that caused a modest increase of mature miR-21 from the retroviral vector that we introduced into MCF-7 cells. As a consequence, over-expression of miR-21 alone did not disrupt morphogenesis of MCF-7 cells.

KEY RESEARCH ACCOMPLISHMENTS

We established a protocol to profile miRNA expression in rBM 3-D culture. We provided the first comparison of miRNA profiles between non-invasive and invasive breast cancer cells, which contained necessary information to explore the role of miRNAs in morphogenesis of mammary epithelial cells. Our in-depth analysis suggested that miR-21 and the miR-200 family are crucial to morphogenesis and cancer progression of the mammary epithelium.

REPORTABLE OUTCOMES

Li C, Nguyen HT, Zhuang Y, Lin Y, Flemington EK, Guo W, Guenther J, Burow ME, Morris GF, Sullivan D, Shan B. Post-transcriptional Up-regulation of miR-21 by Type I Collagen. *Mol Carcinog.* 2011 Jul;50(7):563-70. PubMed PMID: 21647970.

Nguyen HT, Li C, Lasky JA, Kantrow SP, Gilbert Morris GF, Deborah Sullivan DE, Shan B. Modeling the Metastasis Promoting Tumor Microenvironment using Extracellular Matrix Three Dimensional Culture. (International Conference for American Thoracic Society, 2010, selected for oral presentation)

CONCLUSION

rBM 3-D culture can faithfully recapitulate *in vivo* properties of the mammary epithelium. The gene expression signature from the rBM 3-D cultures of breast cancer cells holds prognostic value for breast cancer. Likewise, we provided the first miRNA signature of breast cancer cells in rBM 3-D culture, which can probably serve as a prognostic indicator. We demonstrate proof of principle that ECM modulates miRNA expression and deregulated miRNA expression by the tumor promoting ECM contributes to the aggressiveness of breast cancer, which will pave the road for exploration of miRNA targeting strategies.

REFERENCES

1. Weigelt, B., and Bissell, M. J. (2008) *Semin Cancer Biol* **18**, 311-321
2. Verghese, E. T., Hanby, A. M., Speirs, V., and Hughes, T. A. (2008) *J Pathol* **215**, 214-221
3. Paszek, M. J., Zahir, N., Johnson, K. R., Lakins, J. N., Rozenberg, G. I., Gefen, A., Reinhart-King, C. A., Margulies, S. S., Dembo, M., Boettiger, D., Hammer, D. A., and Weaver, V. M. (2005) *Cancer Cell* **8**, 241-254

APPENDICES

Appendices A & B are the published and submitted manuscript that were supported by this award.

SUPPORTING DATA

All figures/tables are labeled and described in Appendices A & B.

Appendix A

MOLECULAR CARCINOGENESIS 50:563–570 (2011)

BRIEF COMMUNICATION

Post-Transcriptional Up-Regulation of miR-21 by Type I Collagen

Cui Li,[1] Hong T. Nguyen,[2] Yan Zhuang,[2] Yi Lin,[3] Erik K. Flemington,[4] Weichao Guo,[2] James Guenther,[4] Matthew E. Burow,[2] Gilbert F. Morris,[4] Deborah Sullivan,[5] and Bin Shan[2]*

[1]*Key Laboratory of Cancer Proteomics of Chinese Ministry of Health, Xiangya Hospital, Central South University, Hunan, China*
[2]*Department of Medicine, Tulane University School of Medicine, New Orleans, Louisiana*
[3]*Department of Obstetrics and Gynecology, Institute of Obstetrics and Gynecology, Renji Hospital, School of Medicine, Shanghai Jiaotong University, Shanghai, China*
[4]*Department of Pathology, Tulane University School of Medicine, New Orleans, Louisiana*
[5]*Department of Microbiology, Tulane University School of Medicine, New Orleans, Louisiana*

Composition of extracellular matrix (ECM) is crucial to the establishment and maintenance of epithelial apical-basolateral polarity. Increased ECM rigidity caused by deposition of fibrillar collagen, for example, collagen type I (Col-1), promotes loss of epithelial polarity and tumor progression. microRNAs are small non-coding RNAs that regulate gene expression and fundamental cellular processes. The current study explored a link between microRNAs and Col-1 using organotypic three-dimensional culture in which epithelial cells are embedded within Matrigel, a mimic of basement membrane matrix (Matrigel 3-D). Matrigel 3-D culture of A549, MCF-7, and mK-ras-LE cells (lung and mammary epithelial cell lines) gave rise to acinus, an in vitro equivalent of apical-basolateral polarity that consists of a polarized monolayer of epithelial cells facing a central lumen. Supplementation of Col-1 disrupted acinus. Moreover, Col-1 up-regulated the expression of miR-21, a well-documented oncogenic microRNA, via a post-transcriptional mechanism. Similar post-transcriptional up-regulation of miR-21 correlated with deposition of Col-1 in a murine model of lung fibrogenesis. In summary, our findings link altered ECM composition/rigidity and the expression of oncogenic microRNAs. The current study also suggests a novel post-transcriptional mechanism for regulation of miR-21 expression at maturation from pre-miR-21 to mature miR-21.

Key words: microRNA; extracellular matrix; organotypic culture

INTRODUCTION

The biophysical and biochemical properties of extracellular matrix (ECM) within the basement membrane are essential for homeostasis of epithelial apical-basolateral polarity [1,2]. Recent advances highlight the effects of ECM within the tumor microenvironment on cancer progression. Epidemiological studies have revealed a link between breast cancer and elevated mammary density, an X-ray reflection of the rigid and fibrotic tumor microenvironment [3]. The tumor promoting activity of the fibrotic tumor microenvironment is validated experimentally in that deposition of fibrillar collagen, such as collagen type I (Col-1), and a consequent increase in ECM rigidity promotes loss of epithelial polarity and cancer progression [4–6]. As proven by these studies and many others, three-dimensional organotypic culture using basement membrane matrix mimics (Matrigel as its commercial brand, Matrigel 3-D) is a valuable tool to examine the ECM-derived signaling in cancer progression [7].

microRNAs (miRNAs) are small non-coding RNAs that regulate gene expression, often via complementarity with its target sequences within 3′ untranslated region (3′ UTR) of a mRNA [8]. Profiling miRNAs in human cancer specimens and cell lines reveals a growing number of tumorigenic miRNAs [9]. Elevated expression of miR-21 is one of the miRNA signature of human solid tumors [10]. miR-21 can be transcriptionally up-regulated by several cancer-promoting signaling pathways, such as IL-6, AP-1, and androgen receptor [11–13]. TGF-β and BMP signaling up-regulates miR-21 post-transcriptionally via SMAD-promoted processing of pri-miR-21 to pre-miR-21 in vascular smooth muscle cells [14]. Several validated targets of miR-21 further

Additional Supporting Information may be found in the online version of this article.

Abbreviations: ECM, extracellular matrix; Col-1, collagen type 1; Matrigel 3-D, matrigel three-dimensional culture; miRNAs, microRNAs; PDCD4, programmed cell death 4; qRT-PCR, quantitative RT-PCR; GFP, green fluorescent protein.

*Correspondence to: Department of Medicine, Tulane School of Medicine, 1430 Tulane Ave. SL-9, New Orleans, LA 70112.

Received 21 April 2010; Revised 13 December 2010; Accepted 24 December 2010

DOI 10.1002/mc.20742

Published online 11 February 2011 in Wiley Online Library (wileyonlinelibrary.com).

strengthen the oncogenic function of miR-21. For instance, miR-21 targets programmed cell death 4 (PDCD4) and phosphatase and tensin homologue (PTEN) to inhibit apoptosis and promote survival of cancer cells [15,16].

Because of the established roles for rigid ECM and miRNAs in tumor initiation/progression, the current study explored a link between Col-1 deposition in the ECM and expression of miRNAs using 3-D organotypic culture.

MATERIALS AND METHODS

Reagents and Plasmids

Matrigel and Col-1 were purchased from BD Biosciences, Bedford, MD and Sigma, St. Louis, MO, respectively. A 314 nucleotide fragment of pri-miR-21 was inserted in the pMSCV-Puro-GFP retroviral vector (pMSCV-pri-miR-21) as previously described [17]. A pre-miR-21 (the 72 nucleotide stem-loop) expressing vector (pCMV-pre-miR-21) is a kind gift from Dr. Bryan Cullen at Duke University [18]. The antibodies specific for PDCD4 (CS-9535) and β-actin (CS-4970) were purchased from Cell Signaling, Danvers, MA. The DICER-specific antibody (ab-13052) was purchased from Abcam, Cambridge, MA.

Cell Culture and Three-Dimensional Organotypic Culture

A549, a human lung adenocarcinoma cell line was cultured in DMEM as previously described [19]. MCF-7N, N variant of the MCF-7 human breast adenocarcinoma cell line, and its apoptosis resistant derivative MCF-7TN were cultured as described elsewhere [20]. mK-ras-LE, a murine lung epithelial cell line established from a lung tumor bearing *K-ras*^{LA1} mouse, was cultured in RPMI-1640 [21]. Matrigel 3-D culture was carried out as described elsewhere [5,6]. Briefly, the cells were embedded in Matrigel ± Col-1 (1.5 mg/ml) and formation of acinus was monitored for 12 d prior to harvest for RNA or protein analysis.

Transient Transfection and Retroviral Transduction

As previously described, transient and stable ectopical expression of miR-21 precursors was accomplished by transfection and retroviral transduction, respectively [17].

RNA Extraction, Quantitative RT-PCR, and miRNA Array

Total cell RNA was extracted using Trizol (Invitrogen, Carlsbad, CA) and the expression of miR-21 and its precursors was determined using quantitative RT-PCR (qRT-PCR) as previously described [17]. Briefly, total RNA was poly-adenylated and reverse-transcribed using the NCode miRNA First Strand Synthesis kit (Invitrogen) according to the manufacturer's instructions. The resulting cDNA was subjected to quantitative PCR (qRT-PCR) using the NCode universal reverse primer in conjunction with a miR-21-specific forward primer. The values of miR-21 were normalized to that of U6. The sequences of all the primers employed were listed in the Supplementary Table 1. miRNA array analysis on total cell RNA was provided by LC Sciences, Houston, TX (miRBase version 14).

Immunoblots

Total cell protein was extracted from cell colonies isolated from Matrigel ± Col-1 3-D culture using Laemmli buffer as described elsewhere [7]. The expression of the proteins of interest was determined using immunoblots as previously described [19].

Murine Model of Lung Fibrogenesis

To induce lung fibrogenesis, C57BL/6 mice were administered with recombinant adenoviruses encoding either the control green fluorescent protein (GFP-Adv) or active recombinant TGF-β1 (TGF-β1-Adv) at 5×10^8 pfu/mouse as previously described [22,23]. Deposition of Col-1 was evaluated on day 14 post-exposure using Trichrome staining and quantitative RT-PCR.

RESULTS

To model deposition of Col-1 in vitro, we employed Matrigel 3-D organotypic culture with or without supplementation of Col-1 as previously described [5,6]. Matrigel alone mimics the in vivo ECM rigidity surrounding a normal mammary gland, whereas supplementation of Col-1 substantially increases the ECM rigidity and disrupts acinus, a cellular sphere with a central lumen that is an in vitro equivalent of apical-basolateral polarity [5]. We chose A549, MCF-7N, and mK-ras-LE cells because of their ability to form acinus in Matrigel 3-D [Figure 1A(1, 3, and 5) and Supplementary Figure 1]. It is noteworthy that mK-ras-LE formed smaller acinus than A549 and MCF-7N. mK-ras-LE cells express lung epithelial cell markers E-cadherin and surfactant protein-C, but not N-cadherin, a mesenchymal cell marker (data not shown). In all three cell lines, acinus were disrupted when cultured in Matrigel + Col-1 3-D where ECM rigidity is expected to be twice as much as that in Matrigel 3-D [Figure 1A(2, 4, and 6) and Supplementary Figure 1] [5]. The disrupted acinus featured loss of the central lumen and irregular cell clusters with finger-like protrusions, a phenomenon that is indicative of loss of epithelial polarity and acquisition of invasive/metastatic potential [5,6]. E-cadherin is one of the most important markers and regulators of acinus in organotypic culture [2]. Thus, we examined the expression of E-cadherin in Matrigel ± Col-1 3-D cultures of mK-ras-LE, A549, and MCF-7N cells. Consistent with disruption of acinus, the protein levels of E-cadherin in Matrigel + Col-1 3-D was substantially reduced as measured by immunoblots and immunofluorescence (Figure 1B and Supplementary Figure 1B). Moreover, the residual expression of E-cadherin

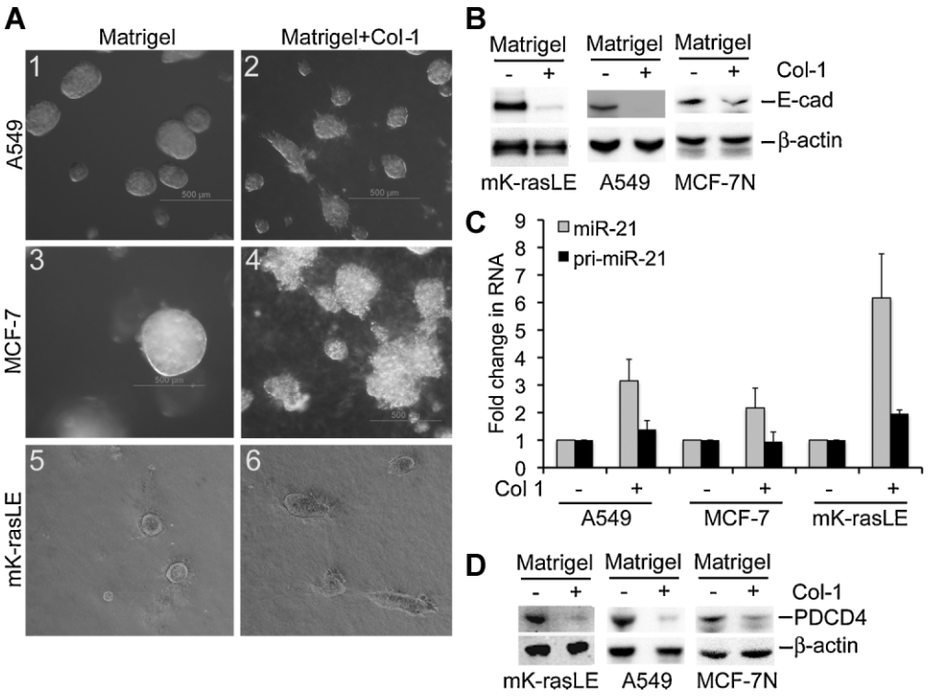

Figure 1. Col-1-mediated up-regulation of miR-21 expression in Matrigel 3-D culture. A549, MCF-7, and mK-ras-LE cells were cultured in Matrigel 3-D culture (Matrigel) with or without supplementation of Col-1 (1.5 mg/ml, Matrigel + Col-1) for 12 d. (A) Morphogenesis of the culture was monitored using a phase-contrast microscope. Representative images of each culture on day 12 are presented. (B) The protein levels of E-cadherin were determined in total cell lysates collected from mK-ras-LE, A549, and MCF-7N cells in Matrigel ± Col-1 3-D using immunoblots. The immunoblots are representative of two independent experiments. (C) The expression of pri-miR-21 and miR-21 was determined using qRT-PCR. A fold change of pri-miR-21 or miR-21 in Matrigel + Col-1 3-D over that in Matrigel 3-D was obtained after normalization to the house keeping gene 36B4 (for pri-miR-21) or U6 (for miR-21) and by setting the values from Matrigel 3-D to one. The results were presented as mean ± standard deviations obtained from three independent cultures. (D) The protein levels of PDCD4 were determined in total cell lysates collected from mK-ras-LE, A549, and MCF-7N cells in Matrigel ± Col-1 3-D using immunoblots. The immunoblots represented two independent experiments.

in Matrigel + Col-1 3-D featured diffuse distribution in mK-ras-LE cells, whereas an intercellular membrane staining pattern of E-cadherin was predominant in Matrigel 3-D, which indicated intact intercellular adhesion and apical-basolateral epithelial polarity (Supplementary Figure 1B).

The expression of mature miR-21 (hereafter referred to as miR-21) was compared between Matrigel ± Col-1 3-D using quantitative qRT-PCR [17]. Supplementation of Col-1 caused a substantial increase in miR-21 over that in Matrigel 3-D as A549, MCF-7, and mK-ras-LE cells displayed three-, two-, and sixfold increase in miR-21, respectively (Figure 1C). We then questioned whether the increase in miR-21 resulted from transcriptional activation. In contrast to the substantial increase in miR-21, we observed modest to minimal alteration in the expression of pri-miR-21 in Matrigel + Col-1 3-D (Figure 1C). When the expression of pre-miR-21 was determined using qRT-PCR with primers priming pri-miR21 and pre-miR-21 followed up by the equation pre-miRNA $= 2^{-C_T(\text{pri-miRNA+pre-miRNA})} - 2^{-C_T\text{pri-miRNA}}$ [24], pre-miR-21 remained largely unchanged in the presence of Col-1 (Supplementary Figure 2). In accord with an increase in miR-21, the protein levels of PDCD4, one of the validated miR-21 targets, were substantially lower in Matrigel + Col-1 3-D culture of mK-ras-LE, A549, and MCF-7N cells than that in Matrigel 3-D (Figure 1D).

We then questioned whether elevated expression of miR-21 was one of a panel of miRNAs that were selectively regulated by Col-1 or merely a reflection of global increase in miRNAs. miRNA arrays were carried out on RNA samples collected from mK-ras-LE cells in Matrigel ± Col-1 3-D. As advised by the service provider, we limited our analysis to the miRNAs with reliable measurement as defined by values greater than 500 in at least one culture condition. Twenty-six miRNAs out of 73 eligible miRNAs were differentially expressed between Matrigel ± Col-1 3-D cultures (Figure 2A, a change greater than twofold, and a P-value < 0.05, $n = 3$). Fourteen miRNAs were up-regulated while 12 miRNAs were down-regulated. A large portion of the up-regulated miRNAs possess tumor-promoting properties. In addition to miR-21, members of the oncogenic

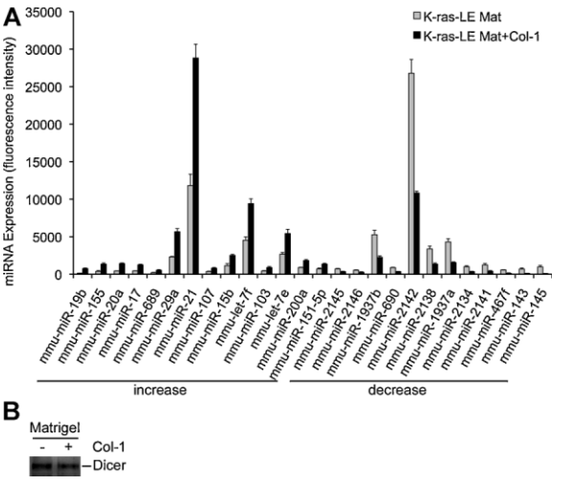

Figure 2. Col-1-induced differential expression of miRNAs in Matrigel 3-D culture. (A) miRNA arrays were carried out on total cell RNA collected from mK-ras-LE cells in Matrigel ± Col-1 cultures. The miRNAs that were altered by Col-1 were defined as (1) values greater than 500 in at least one culture condition; (2) greater than twofold difference; (3) a *P*-value smaller than 0.05 as determined by unpaired two tail Student's *t*-test. The results were presented as means and standard deviations from three independent experiments. (B) The culture condition was similar to part A. The cell lysates were collected from the cell colonies extracted from the culture. The protein levels of DICER were determined using immunoblots. The loading control β-actin is presented in Figure 1B. The results represented two independent experiments.

miR-17-92 cluster (miR-17, miR-19b, and miR-20a), and miR-155 were substantially up-regulated [10,25]. However, several miRNAs with tumor suppressive activity were also up-regulated modestly, such as let-7f/e and miR-200a [26]. Among the decreased miRNAs, the miR-143–145 cluster is tumor suppressive miRNAs while relevance of the remaining miRNAs is unclear [27]. In addition, the total readings of miRNAs were nearly identical between the two culture conditions (229 944 in Matrigel 3-D vs. 238 299 in Matrigel + Col-1 3-D). We further compared the expression of DICER, a central component of the pre- to mature miRNA processing machinery between the two culture conditions. Consistent with nearly identical expression of total miRNAs, the protein levels of DICER were comparable between the two culture conditions (Figure 2B).

To confirm existence of a post-transcriptional regulation of miR-21, we generated A549 and MCF-7N variants that ectopically expressed a fragment of human pri-miR-21 from a retroviral vector pMSCV-Puro-GFP as previously described [17]. The expression of pri-miR-21 and miR-21 were compared between the variants transduced with the backbone pMSCV-Puro-GFP vector (A549/MCF-7vec) and the pMSCV-Puro-GFP-miR-21 vector (A549/MCF-7miR-21). Ectopic expression of the miR-21 precursor in A549/MCF-7miR-21 resulted in a five- to sixfold increase in pri-miR-21 over that in A549/MCF-7vec, whereas miR-21 exhibited no change in A549/MCF-7miR-21 when compared to A549/MCF-7vec (Figure 3A). On the other hand, ectopic expression of two other precursors for miR-155 and miR-17–92 cluster yielded robust expression of the corresponding mature forms (data not shown). Transient transfection of A549 cells with pCMV-pre-miR-21 that encodes only pre-miR-21 resulted in 30% decline in miR-21 despite a 140-fold increase in pre-miR-21 (Figure 3B and C) [18]. We speculated that limited maturation of ectopically expressed miR-21 precursor reflected rate-limiting maturation miR-21 precursors due to abundance of the endogenous miR-21 (Figure 2A). We further reasoned that the miR-21 expressing vectors would efficiently produce miR-21 in the cell with low levels of endogenous miR-21. Thus, pCMV-pre-miR-21 and its backbone vector were transfected into MCF-7TN cells, an apoptosis resistant derivative of MCF-7N in which miR-21 expression was nearly silenced (Supplementary Figure 3A). The vector-derived production of miR-21 was only observed in MCF-7TN, which reached to around 30% of that in MCF-7N (Figure 3D). The RNA levels of pre-miR-21 (the sum of endogenous and exogenous) were comparable between MCF-7N and MCF-7TN transfected with pCMV-pre-miR-21 (Supplementary Figure 3B). These findings indicate that production of miR-21 from the vector derived pre-miR-21 is at least in part dictated by the levels of endogenous miR-21.

We then set to determine whether Col-1 deposition correlated with an increase in miR-21 in a murine model of lung fibrogenesis induced by TGF-β1-Adv as previously described [22,23]. Deposition of Col-1 in the mouse lung exposed to TGF-β1-Adv was confirmed using Trichrome staining, a specific staining for collagen as well as qRT-PCR for Col-1 (Figure 4A and B). Similar to our in vitro findings, deposition of Col-1 in the mouse lung correlated with a nearly threefold increase in miR-21 over that in the mice exposed to the control GFP (GFP-Adv) and was accompanied by the absence of any congruent alteration in pri-miR-21 (Figure 4C and D). These findings demonstrated a correlation between deposition of Col-1 and post-transcriptional up-regulation of miR-21 in vivo.

DISCUSSION

It is well documented that elevated ECM rigidity promotes tumor progression [4–6]. In the organotypic culture that we employed, addition of Col-1 to Matrigel is expected to increase ECM rigidity by nearly two times [5]. In addition to miR-21, Col-1 alters the expression of several miRNAs bearing well-documented relevance to cancer, such as increased expression of the tumorigenic miR-17–92 cluster and miR-155, and reduced expression of the tumor

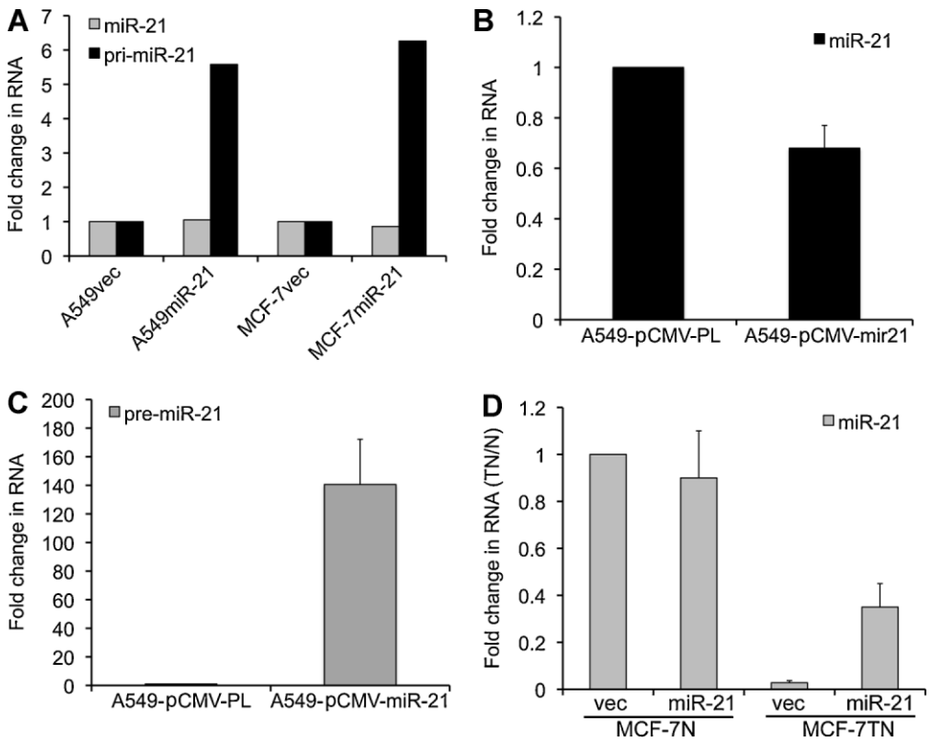

Figure 3. Rate-limiting maturation of the miR-21 precursors. (A) A549 and MCF-7 derivatives were generated by transduction of the two cell lines with either a retroviral vector expressing a fragment of pri-miR-21 (A549/MCF-7miR-21) or the backbone vector (A549/MCF-7vec). The expression of pri-miR-21 and mature miR-21 was determined using qRT-PCR. A fold change of either pri-miR-21 or miR-21 in A549/MCF-7miR-21 over that in A549/MCF-7vec was determined as described in Figure 1. The results presented were average from two independent experiments. (B) A549 cells were transfected with a pCMV vector expressing pre-miR-21 (A549-pCMV-miR-21) or the backbone vector (A549-pCMV-PL). Total cell RNA was extracted at 72 h after transfection. The expression of miR-21 was determined using qRT-PCR as described in part A. (C) Similar to (B) except that the vector derived expression of pre-miR-21 was determined using a pair of primers that amplify both pri- and pre-miR-21. (D) MCF-7N and MCF-7TN cells were transfected with pCMV-pre-miR-21 (pre-miR-21) or its backbone vector (vec). The expression of miR-21 was determined using qRT-PCR. A fold change in RNA levels of miR-21 was obtained by setting the values from MCF-7N transfected with the backbone vector to one. The results were presented as means and standard deviations obtained from three independent transfections.

suppressive miR-143–145 cluster (Figure 2A) [25,27]. Up-regulated miR-21 correlates with deposition of Col-1 in lung fibrogenesis (Figure 4). TGF-β1 may directly up-regulate miR-21 in the lung because TGF-β1 up-regulates DROSHA-mediated pri- to pre-miR-21 processing in human vascular smooth muscle cells [14]. We reason that Col-1, at least in part, contributes to miR-21 up-regulation in lung fibrogenesis because TGF-β1 alone does not alter the expression of miR-21 in either A549 cells or primary culture of human lung fibroblasts which are surrogate of alveolar epithelial cells and fibroblasts, two major cell types in lung fibrogenesis, respectively. Up-regulated expression of miR-21 is not consequent of a global alteration in miRNA expression because the total reading of miRNAs and the protein levels of DICER are comparable between Matrigel ± Col-1 3-D cultures (Figure 2). These findings implicate that Col-1 selectively regulates the expression of a panel of miRNAs to promote cancer progression.

Elevated expression of miR-21 is correlated with decreased expression of PDCD4, a miR-21 target that can promote apoptosis, a key mechanism in formation of central lumen in acinus (Figure 1C) [1,2,16]. Our study warrants further investigation of whether suppression of PDCD4 expression by Col-1 is miR-21 mediated and in turn promotes apoptosis resistance and loss of the central lumen. Given the profound change in miRNA profile caused by Col-1 and the complexity of homeostasis of epithelial polarity, it is highly likely that each individual Col-1-regulated miRNA modulates only certain aspect/s of acinus (Figure 2A). The full spectrum disruption of acinus may require collective efforts of miR-21 and other Col-1 responsive miRNAs, such as miR-17–92 and miR-143–145 clusters. Besides PDCD4, E-cadherin is down-regulated by Col-1 (Figure 1B). However, it is unclear whether such a down-regulation is miRNA-mediated. The 3′ UTR of the E-cadherin transcript is predicted to harbor only one miR-9 target site. miR-9 expression is not altered

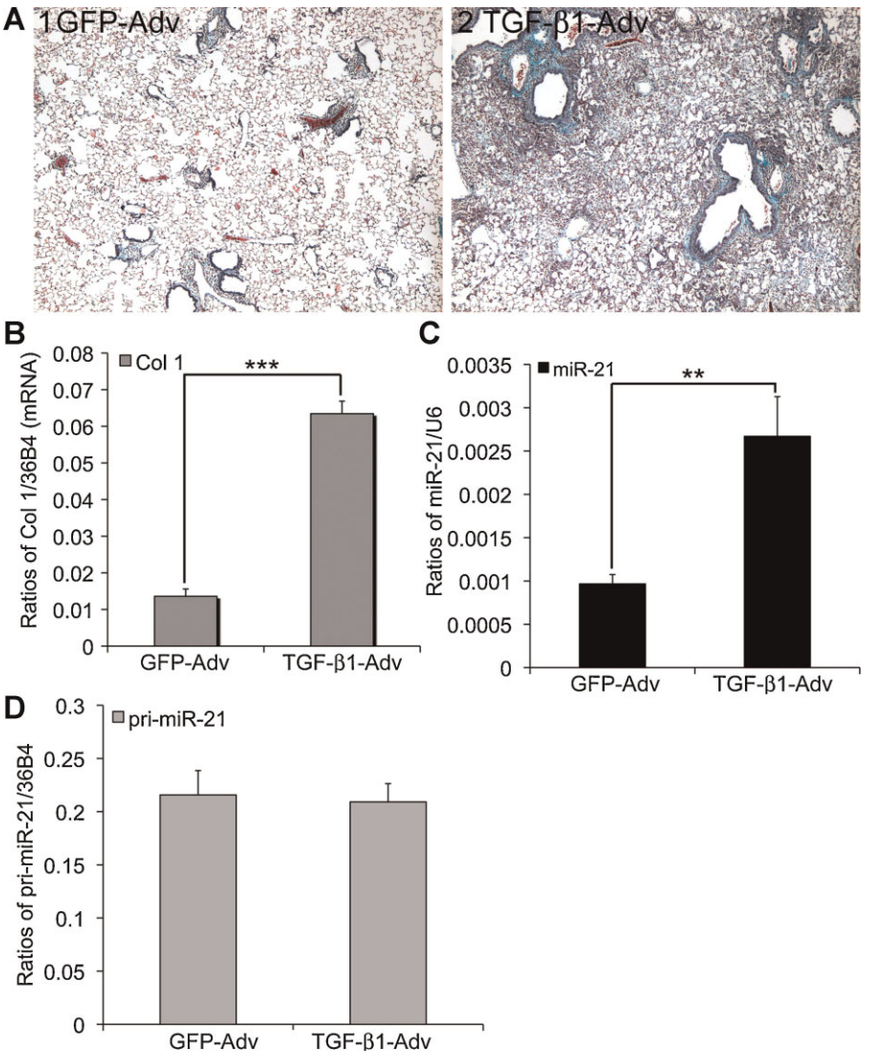

Figure 4. Post-transcriptional up-regulation of the expression of miR-21 in mouse lung fibrogenesis. Lung fibrogenesis was induced by exposure of the mouse lung to either TGF-β1-Adv or GFP-Adv (3×10^8 pfu) for 14 d. (A) Deposition of collagen was assessed using blue Trichrome staining. Representative histology was presented. (B) Total RNA was extracted from the lungs of the exposed mice. The expression of Col-1 was determined using qRT-PCR. The ratios of Col-1 versus the house keeping gene 36B4 were compared across the groups. (C,D) Similar to B except that the ratios of the pri- or mature miR-21 versus their corresponding control 36B4 or U6 were compared across the groups. The results were presented as mean ± standard deviations from 7 mice per group. *** and ** denote a *P*-value smaller than 0.001 and 0.01, respectively as determined using unpaired two-tailed Student's *t*-test (Prizm).

by Col-1 in mK-ras-LE cells (Figure 2A). miR-200 family activates the expression of E-cadherin by targeting ZEB1/2, the transcriptional repressor of the E-cadherin gene [26]. Intriguingly, expression of the members of miR-200 family is not repressed by Col-1 (Figure 2A and unpublished observations).

miR-21 expression can be regulated both transcriptionally and post-transcriptionally. AP-1 mediates activation of pri-miR-21 expression by the carcinogenic phorbol 12-myristate 13-acetate via multiple AP-1 and PU.1 binding sites in the miR-21 promoter in human promyelocytic cells [13]. The tumor-promoting cytokine IL-6 activates expression of pri-miR-21 in multiple myeloma cells via the transcription factor STAT3 [12]. Post-transcriptionally, pri-miR-21 to pre-miR-21 processing is promoted by SMAD and inhibited by the NF90-NF45 complex [14,28]. These mechanisms might contribute to Col-1-mediated up-regulation of miR-21, either directly or indirectly. In addition, our data suggest a third layer of regulation at the maturation from pre-miR-21 to miR-21 because Col-1 up-regulates only miR-21, but not its precursors. Moreover, ectopical expression of pre-miR-21, fails to produce miR-21

(Figure 3). In MCF-7TN cells with low endogenous level of miR-21, ectopical expression of pre-miR-21 can produce miR-21 and partially restore miR-21 expression to around 30% of the endogenous miR-21 levels in MCF-7N (Figure 3D and Supplementary Figure 3B). Because expression of miR-21 from exogenous pre-miR-21 is dictated by the levels of endogenous miR-21, it is plausible that a sensing system exists in the cell to prevent excessive production of miR-21 by limiting maturation of pre-miR-21 to miR-21. Appealing hypotheses to be tested are whether nuclear export of pre-miR-21 is tightly regulated and whether Col-1 impairs such a regulation to up-regulate miR-21 post-transcriptionally. It is noteworthy that MCF-7TN cells are more tumorigenic than MCF-7N (Burow ME, personal communication), which raises the possibility that miR-21 can be dispensable for cancer in certain contexts. In line with this speculation, MCF-7TN cells exhibited disrupted acinus and reduced expression of E-cadherin and PDCD4 in Matrigel 3-D culture (Supplementary Figure 4). These findings implicate that loss of miR-21 mediated suppression of PDCD4 can be compensated under certain conditions.

ECM signals through heterodimers of integrins on the cell surface. $\alpha 2\beta 1$ is the most well-characterized receptor for Col-1 and mediates tumor promoting effects of Col-1 in prostate and pancreatic cancer cells [29–31]. Profound alteration of miRNA expression by Col-1 in organotypic culture provides an ideal platform to investigate integrin-regulated expression of miRNAs in the context of cancer progression (Figures 1 and 2). Generation of integrin deficient variants is underway in our laboratory to define the roles for integrins in miRNA response to Col-1.

Because miR-21 has been identified as one of the signature miRNAs of human solid tumors and elevated miR-21 expression correlates with deposition of Col-1 in vitro and in vivo (Figures 1 and 3), our results implicate miR-21 as a biomarker and potential therapeutic target of the cancer cell response to increased ECM rigidity [10]. Our findings warrant further investigation to define the molecular mechanisms for post-transcriptional up-regulation of miR-21 by Col-1 and the role of miR-21 in epithelial polarity.

ACKNOWLEDGMENTS

This work was supported in part by LEQSF (2008-10)-RD-A-26, Office of Naval Research BAA # 05-001, and DOD BC085516 awarded to BS, and by NCI CA132603 awarded to BS, GM, and DS. H. T. Nguyen and J. Guenther are supported in part by Developmental Funds of the Tulane Cancer Center. We are grateful to Dr. Patricia Sime for the expression vectors that encoding GFP-Adv and TGF-β1-Adv. We are also grateful to Ms. Carol Gadwaw for her excellent technical assistance.

REFERENCES

1. Weigelt B, Bissell MJ. Unraveling the microenvironmental influences on the normal mammary gland and breast cancer. Semin Cancer Biol 2008;18:311–321.
2. Bryant DM, Mostov KE. From cells to organs: Building polarized tissue. Nat Rev Mol Cell Biol 2008;9:887–901.
3. Boyd NF, Martin LJ, Yaffe M, Minkin S. Mammographic density. Breast Cancer Res 2009;11:S4.
4. McCormack VA, dos Santos Silva I. Breast density and parenchymal patterns as markers of breast cancer risk: A meta-analysis. Cancer Epidemiol Biomarkers Prev 2006;15:1159–1169.
5. Paszek MJ, Zahir N, Johnson KR, et al. Tensional homeostasis and the malignant phenotype. Cancer Cell 2005;8:241–254.
6. Levental KR, Yu H, Kass L, et al. Matrix crosslinking forces tumor progression by enhancing integrin signaling. Cell 2009;139:891–906.
7. Lee GY, Kenny PA, Lee EH, Bissell MJ. Three-dimensional culture models of normal and malignant breast epithelial cells. Nat Methods 2007;4:359–365.
8. Trang P, Weidhaas JB, Slack FJ. MicroRNAs as potential cancer therapeutics. Oncogene 2008;27:S52–S57.
9. Verghese ET, Hanby AM, Speirs V, Hughes TA. Small is beautiful: MicroRNAs and breast cancer-where are we now? J Pathol 2008;215:214–221.
10. Volinia S, Calin GA, Liu CG, et al. A microRNA expression signature of human solid tumors defines cancer gene targets. Proc Natl Acad Sci USA 2006;103:2257–2261.
11. Ribas J, Ni X, Haffner M, et al. miR-21: An androgen receptor-regulated microRNA that promotes hormone-dependent and hormone-independent prostate cancer growth. Cancer Res 2009;69:7165–7169.
12. Loffler D, Brocke-Heidrich K, Pfeifer G, et al. Interleukin-6 dependent survival of multiple myeloma cells involves the Stat3-mediated induction of microRNA-21 through a highly conserved enhancer. Blood 2007;110:1330–1333.
13. Fujita S, Ito T, Mizutani T, et al. miR-21 Gene expression triggered by AP-1 is sustained through a double-negative feedback mechanism. J Mol Biol 2008;378:492–504.
14. Davis BN, Hilyard AC, Lagna G, Hata A. SMAD proteins control DROSHA-mediated microRNA maturation. Nature 2008;454:56–61.
15. Meng F, Henson R, Wehbe-Janek H, Ghoshal K, Jacob ST, Patel T. MicroRNA-21 regulates expression of the PTEN tumor suppressor gene in human hepatocellular cancer. Gastroenterology 2007;133:647–658.
16. Frankel LB, Christoffersen NR, Jacobsen A, Lindow M, Krogh A, Lund AH. Programmed cell death 4 (PDCD4) is an important functional target of the microRNA miR-21 in breast cancer cells. J Biol Chem 2008;283:1026–1033.
17. Yin Q, McBride J, Fewell C, et al. MicroRNA-155 is an Epstein-Barr virus-induced gene that modulates Epstein-Barr virus-regulated gene expression pathways. J Virol 2008;82:5295–5306.
18. Zeng Y, Cullen BR. Sequence requirements for micro RNA processing and function in human cells. RNA 2003;9:112–123.
19. Shan B, Yao TP, Nguyen HT, et al. Requirement of HDAC6 for transforming growth factor-beta1-induced epithelial-mesenchymal transition. J Biol Chem 2008;283:21065–21073.
20. Weldon CB, Parker AP, Patten D, et al. Sensitization of apoptotically-resistant breast carcinoma cells to TNF and TRAIL by inhibition of p38 mitogen-activated protein kinase signaling. Int J Oncol 2004;24:1473–1480.
21. Johnson L, Mercer K, Greenbaum D, et al. Somatic activation of the K-ras oncogene causes early onset lung cancer in mice. Nature 2001;410:1111–1116.

22. Sime PJ, Xing Z, Graham FL, Csaky KG, Gauldie J. Adenovector-mediated gene transfer of active transforming growth factor-beta1 induces prolonged severe fibrosis in rat lung. J Clin Invest 1997;100:768–776.
23. Lakatos HF, Burgess HA, Thatcher TH, et al. Oropharyngeal aspiration of a silica suspension produces a superior model of silicosis in the mouse when compared to intratracheal instillation. Exp Lung Res 2006;32:181–199.
24. Schmittgen TD, Jiang J, Liu Q, Yang L. A high-throughput method to monitor the expression of microRNA precursors. Nucleic Acids Res 2004;32:e43.
25. Mendell JT. miRiad roles for the miR-17-92 cluster in development and disease. Cell 2008;133:217–222.
26. Gregory PA, Bert AG, Paterson EL, et al. The miR-200 family and miR-205 regulate epithelial to mesenchymal transition by targeting ZEB1 and SIP1. Nat Cell Biol 2008;10:593–601.
27. Volinia S, Galasso M, Costinean S, et al., Reprogramming of miRNA networks in cancer and leukemia. Genome Res 2010;20:589–599.
28. Sakamoto S, Aoki K, Higuchi T, et al. The NF90-NF45 complex functions as a negative regulator in the microRNA processing pathway. Mol Cell Biol 2009;29:3754–3769.
29. Xu Y, Gurusiddappa S, Rich RL, et al. Multiple binding sites in collagen type I for the integrins alpha1beta1 and alpha2-beta1. J Biol Chem 2000;275:38981–38989.
30. Grzesiak JJ, Bouvet M. The alpha2beta1 integrin mediates the malignant phenotype on type I collagen in pancreatic cancer cell lines. Br J Cancer 2006;94:1311–1319.
31. Hall CL, Dubyk CW, Riesenberger TA, Shein D, Keller ET, van Golen KL. Type I collagen receptor (alpha2beta1) signaling promotes prostate cancer invasion through RhoC GTPase. Neoplasia 2008;10:797–803.

Appendix B

The microRNA expression associated with morphogenesis of breast cancer cells in three-dimensional organotypic culture

HONG T. NGUYEN[1]*, CUI LI[2]*, ZHEN LIN[3], YAN ZHUANG[1], ERIK K. FLEMINGTON[3], MATTHEW E. BUROW[1], YI LIN[4], AND BIN SHAN[1§]

[1]Department of Medicine, Tulane University School of Medicine, 1430 Tulane Avenue, New Orleans, LA 70112, USA
[2]Key Laboratory of Cancer Proteomics of Chinese Ministry of Health, Xiangya Hospital, Central South University, Hunan 41008, China
[3]epartment of Pathology, Tulane University School of Medicine, 1430 Tulane Avenue, New Orleans, LA 70112, USA
[4]Department of Obstetrics and Gynecology, Institute of Obstetrics and Gynecology, Renji Hospital, School of Medicine, Shanghai Jiaotong University, Shanghai, China

*Correspondence author.

*These two authors contributed equally to the manuscript.

Email addresses:
HTN: hnguyen9@tulane.edu
CL: pwblicui@hotmail.com
ZL: zlin@tulane.edu
YZ: yzhuang1@tulane.edu
EKF: eflemin@tulane.edu
MEB: mburow@tulane.edu
YL: yilinonline@sohu.com
BS: bshan@tulane.edu

Abstract

Three-dimensional organotypic culture using reconstituted basement membrane matrix Matrigel (rBM 3-D) is an indispensable tool to characterize morphogenesis of mammary epithelial cells and to elucidate the tumor-modulating actions of extracellular matrix (ECM). microRNAs (miRNA) are a novel class of oncogenes and tumor suppressors. The majority of our current knowledge of miRNA expression and function in cancer cells is derived from monolayer 2-D culture on plastic substratum, which lacks a consideration of the influence of ECM-mediated morphogenesis on miRNAs. In the current study we compared the expression of miRNAs in rBM 3-D and 2-D cultures of the non-invasive MCF-7 and the invasive MDA-MB231 cells. Our findings revealed a profound difference in miRNA profiles between 2-D and rBM 3-D cultures within each cell type. Moreover, rBM 3-D culture exhibited greater discrimination in miRNA profiles between MCF-7 and MDA-MB231 cells than 2-D culture. The disparate miRNA profiles correlated with distinct mass morphogenesis of MCF-7 and invasive stellate morphogenesis of MDA-MB231 cells in rBM 3-D culture. Supplementation of the tumor promoting type I collagen in rBM 3-D culture substantially altered the miRNA signature of mass morphologenesis of MCF-7 cells in rBM 3-D culture. Lastly, overexpression of the differentially expressed miR-200 family member miR429 in MDA-MB231 cells attenuated their invasive stellate morphogenesis in rBM 3-D culture. In summary, we provide the first miRNA signatures of morphogenesis of human breast cancer cells in rBM 3-D culture and warrant further utilization of rBM 3-D culture in investigation of miRNAs in breast cancer.

Key Words: microRNA; three-dimensional organotypic culture; extracellular matrix; breast cancer; morphogenesis.

Introduction

The tumor microenvironment, a newly established crucial determinant in tumorigenesis, is composed of extracellular matrix (ECM), growth factors, and inflammatory cytokines that are produced by the co-evolved neoplastic epithelial cells and associated stromal cells (1, 2). During acquisition of invasive and metastatic competence, cancer cells progress to loose differentiation response to basement membrane matrix (BM), such as a loss of epithelial cell apical-basolateral polarity (3). The three-dimensional organotypic culture using reconstituted basement membrane Matrigel (hereinafter referred to as rBM 3-D) provides an ideal platform to elucidate the molecular mechanisms that mediate the dysregulated morphogenesis during mammary tumorigenesis because rBM 3-D culture faithfully recapitulates many *in vivo* properties of mammary epithelial cells (4-7). Genome wide expression profiling of breast cancer in rBM 3-D culture has established gene expression signatures associated with distinct morphologenesis of breast cancer cell lines with diverse invasive and metastatic properties (8). The clinical significance of the gene expression profiles derived from rBM 3-D culture is confirmed in that the gene expression signature from rBM 3-D culture of breast cancer cells holds prognostic values for patients with breast cancer (9).

microRNAs (miRNAs) are small non-coding RNAs that inhibit gene expression often *via* complementarity with its target sequences within the 3' untranslated region (3' UTR) of a mRNA (10). Profiling miRNAs in human cancer specimens and cell lines reveals a growing number of tumorigenic and tumor suppressive miRNAs (11). Among the tumor suppressive miRNAs, the let-7 family and miR-200 family are frequently silenced in cancer (12). The let-7 family suppresses tumor growth via targeting cell cycle regulators (CDC25A and CDK6), promoters of growth (RAS and c-myc), and early embryonic genes (HMGA2) (13-15). The miR-200 family inhibits epithelial to mesenchymal transition (EMT) via targeting two EMT mediators, E box binding transcription factors ZEB1 and ZEB2, and thereby suppresses invasion and metastasis (16, 17).

Despite the importance of rBM 3-D culture and miRNAs in the research of breast cancer, miRNAs have not been characterized in rBM 3-D culture of breast cancer cells. The current study is aimed to elucidate the biology of miRNAs in morphogenesis of breast cancer cells with diverse invasive and metastatic potentials in rBM 3-D culture.

Materials and Methods

Reagents and Plasmids. Matrigel was purchased from BD Biosciences (Rockville, MD). Cell culture grade type I collagen was purchased from Sigma (St. Louis MO). A human miR-429 expression retroviral vector was generated by inserting the human pre-miR-429 into the pMSCV-puro-GFP-miR backbone vector as we previously described (18). Alexa 594 conjugated filamentous actin (F-actin) binding phalloidin was purchased from Invitrogen (Carlsbad, CA).

Cell Culture and Retroviral Transduction. Two human breast cancer cell lines, MCF-7 cells (N variant) and MDA-MB231 cells were cultured in DMEM (Sigma) as previously described (19, 20). Stable ectopical expression of miR-429 in MDA-MB231 cells was accomplished by retroviral transduction as we previously described (21). Briefly miR-429 expressing and its backbone control retroviral vectors were produced using 293T cells. MDA-MB231 cells were then infected with the retroviruses and the stable transductants were selected and maintained using puromycin containing culture medium.

rBM three dimensional organotypic culture. Overlay rBM 3-D culture was carried out as described elsewhere (4). Briefly, MCF-7 and MDA-MB231 cells were seeded at 2 x 10^5 cells/well in a 6-well cell culture plate that was coated with Matrigel. DMEM culture medium was supplemented with 4% of Matrigel and fresh medium was fed every two days. In the selected rBM 3-D culture of MCF-7 cells, Col-1 (2 μg/ml) was added as described elsewhere (22). The morphology of cell clusters was monitored for 12 days and recorded using an inverse phase contrast microscope equipped with a digital camera based on the time course of morphogenesis of mammary epithelial cells in rBM 3-D culture as established in the previous studies Debnath, 2003 #11}. The cell morphogenesis was also visualized by staining for filamentous actin using Alexa 594 conjugated phalloidin followed by confocal fluorescent microscopy analysis on a Bio-Rad Radiance 2100 system (Hercules, CA), which is an established method to monitor morphogenesis of mammary epithelial cells (8).

RNA Extraction and Analysis of mRNA and miRNA Expression. Total cell RNA was extracted using Trizol (Invitrogen) from 2-D culture when the cells reached ~80% confluence and from rBM 3-D cultures on day 12 after the cells were seeded. Quantitative RT-PCR (qRT-PCR) was carried out to determine the expression of E-cadherin, vimentin, and ZEB2 as previously described (23, 24). The expression of let-7c, and members of miR-200 family (miR-200c, miR-141, and miR-429) was meaured using TaqMan miRNA Assays as we previously described (18). The gene expression was normalized to 36B4 for the protein coding genes and to U6 for the miRNAs, respectively. A fold change of each transcript was obtained by setting the values from the control group to one. All the measurements were repeated on the RNA samples collected from three independent experiments.

miRNA array analysis. LC Sciences (Houston, TX) provided the microRNA expression profiling service using μParaflo® technology and proprietary probe hybridization (Cy3 and Cy5 dendrimer dyes) that enables highly sensitive and specific direct detection of human based on Sanger Institute human miRbase version 14 (894 human miRNAs). The miRNA microarrays of each culture condition were carried out on the RNA samples collected from three independent experiments. As advised by the service provider, any miRNA with a fluorescent intensity value below 100 in all of the compared groups was excluded in the analysis. Multi-array log2 transformation, normalization, t-test, and unsupervised hierarchy clustering analysis (average linkage and a Euclidean distance metric) were carried out using the geWorkbench genomic analysis software suite to identify the differentially expressed miRNAs between any two selected groups

(http://www.geworkbench.org) (25). False Discovery Rate (FDR) was calculated using the Significance Analysis of Microarrays suite (SAM) (26). The miRNAs that carried a greater than 2-fold difference, $P < 0.01$, and FDA < 0.05 between any two compared groups were considered significantly differentially expressed between the two groups.

Statistical analysis. Statistical significance in the values compared between any two selected groups was determined using the unpaired two-tailed Student *T* test (Prizm Version 5). A *P* value < 0.05 was considered significant.

Results

Correlation of miRNA expression and morphogenesis of breast cancer cells. A recent study has uncovered gene expression profiles underlying distinct morphogenesis of breast cancer cell lines with diverse tumorigenic properties in rBM 3-D culture (8). Because miRNAs can modulate expression of the protein coding genes, we profiled miRNA expression underlying distinct morphogenesis of the non-invasive MCF-7 and the invasive MDA-MB231 cells in rBM 3-D culture. As revealed by inverse phase-contrast microscopy and fluorescent staining for F-actin, MCF-7 cells exhibited a mass morphology, a hallmark feature of non-invasive breast cancer cells that was defined by cell clusters with disorganized nuclei, robust cell-cell adhesion, and low frequency of formation of a central lumen, (Figure 1, A1 and B1) (8). In contrast, MDA-MB231 exhibited an invasive stellate morphology, a hallmark feature of invasive breast cancer cells that was defined by disorganized nuclei and elongated cell body with prominent invasive projections that often bridge multiple cell colonies, (Figure 1, A2 and B2) (8). In accordance, MCF-7 cells exhibited epithelial phenotype in 2-D culture, which included high expression of E-cadherin, an epithelial cell marker, and low expression of vimentin, a mesenchymal cell marker (data not shown). On the other hand, MDA-MB231 cells exhibited mesenchymal phenotype in 2-D culture, which included low expression of E-cadherin and high expression of vimentin (data not shown). The differential expression of E-cadherin and vimentin between MCF-7 and MDA-MB231 cells was retained in rBM 3-D culture (data not shown).

To identify the miRNA candidates that discriminated mass and stellate morphogenesis we compared miRNA arrays in 2-D and rBM 3-D cultures of MCF-7 and MDA-MB231 cells. As expected, the miRNA expression profiles exhibited profound difference among diverse culture conditions. In rBM 3-D culture 75 miRNAs were differentially expressed between mass morphology of MCF-7 cells and stellate morphology of MDA-MB231 cells (Figure 1C). Within this panel 61 miRNAs exhibited >2-fold difference between MCF-7 and MDA-MB231 cells with 40 miRNAs being higher and 21 miRNAs being lower in MCF-7 over that MDA-MB231. In 2-D culture 70 miRNAs were differentially expressed between the epithelial phenotype of MCF-7 cells and the mesenchymal phenotype of MDA-MB231 cells (Figure 1D). Within this panel 60 miRNAs exhibited >2-fold difference between MCF-7 and MDA-MB231 cells with 45 being higher and 15 being lower in MCF-7 over MDA-MB231. Because this study was aimed to identify the miRNAs that discriminated mass and stellate morphologies, we identified 29 miRNAs whose expression differed between MCF-7 and MDA-MB231 cells

only in rBM 3-D culture (Table 1). This panel of miRNAs featured a large number of miRNAs with known tumor modulating functions. For instance, two members of the tumor suppressive miR-200 family, miR-141 and miR-429 were higher in MCF-7 than that in MDA-MB231 cells (Table 1) (16, 17). Intriguingly, the tumor suppressive let-7 family in general exhibited a paradoxical lower expression in MCF-7 cells than that in MDA-MB231 cells (Table 1) (13-15). Except for the miRNAs listed in Table 1, the rest of the miRNAs in Figure 1C were commonly differentially expressed between MCF-7 and MDA-MB231 cells regardless of culture conditions, which featured higher expression of the tumor suppressive miR-200c and lower expression of the tumor promoting miR-221/222 cluster in MCF-7 cells than that in MDA-MB231 cells (16, 17, 27). These findings revealed a correlation between miRNA expression and morphogenesis of breast cancer cells in rBM 3-D culture.

We speculated that a disparate response of miRNA expression during transition from 2-D to rBM 3-D culture in MCF-7 and MDA-MB231 cells gave rise to the rBM-3D-specific differential miRNAs between MCF-7 and MDA-MB231 cells. Therefore, we compared the miRNA profiles between 2-D and rBM 3-D cultures within each cell type to identify the rBM 3-D responsive miRNAs. In MCF-7 cells 49 miRNAs were differentially expressed between rBM 3-D and 2-D cultures at a >2-fold difference with 24 miRNAs being higher and 25 miRNAs being lower in rBM 3-D than that in 2-D (Table 2). In MDA-MB231 cells, 28 miRNAs were differentially expressed between 2-D and rBM 3-D cultures at a >2-fold difference with 22 miRNAs being higher and 6 miRNAs being lower in rBM 3-D than that in 2-D (Table 3). Moreover, the majority of the rBM responsive miRNAs were unique to MCF-7 and MDA-MB231 cells except for only 9 rBM 3-D responsive miRNAs that were common to MCF-7 and MDA-MB231 cells (a comparison of Tables 2 and 3, the miRNAs unique to each cell type were in bold format). The miRNAs showing differential response to rBM were likely the miRNAs that mediated mass and stellate morphology. This panel of miRNAs featured two members of miR-200 family, miR-141 and miR-429 that were induced in rBM 3-D culture only in MCF-7, but not MDA-MB231 cells.

Dysregulation of miRNA expression by Col-1 in rBM 3-D culture of MCF-7 cells. The tumor-promoting Col-1 is able to disrupt acinar and mass morphogenesis of mammary epithelial cells in rBM 3-D culture and promote progression of mammary tumorigenesis in mouse models (22, 24, 28). Therefore, we questioned whether Col-1 dysregulated the expression of miRNAs of MCF-7 cells in rBM 3-D. We compared the miRNA profiles of MCF-7 cells in rBM 3-D and rBM 3-D+Col-1. Col-1 altered the expression of 80 miRNAs (Figure 2A). Within this panel, 61 miRNAs exhibited >2-fold difference between rBM 3-D and rBM 3-D+Col-1 with 25 miRNAs being up-regulated and 36 miRNAs being down-regulated by Col-1 (Table 4). Because Col-1 disrupted acinar/mass morphogenesis of MCF-7 cells, we then questioned whether Col-1 dysregulated the expression of the MCF-7-specific rBM responsive miRNAs that were potential miRNA mediators of mass morphogenesis of MCF-7 cells in rBM 3-D culture (Table 2, indicated by bold font). Indeed, the expression of 23 MCF-7-specific rBM responsive miRNAs was dysregulated by Col-1 because the expression profile of these miRNAs was shifted towards the expression profile in 2-D culture (Table 4, indicated by

bold font). This panel of miRNAs featured a decreased expression of 3 members of the miR-200 family, miR-200a, miR-141, and miR-429, and an increased expression of 8 members of the let-7 family (Table 4). This trend was further supported by clustering analysis of miRNA arrays of 2-D, rBM 3-D, and rBM 3-D+Col-1 cultures in that the miRNA profile of rBM 3-D+Col-1 was clustered more proximal to the miRNA profile of 2-D than to that of rBM 3-D (Figure 2B).

Validated expression of the differential miRNAs between MCF-7 and MDA-MB231. Because the expression of the members of the miR-200 and let-7 families differed substantially between MCF-7 and MDA-MB231 cells in rBM 3-D culture, and was dysregulated by Col-1 in MCF-7 cells, we validated the expression of these miRNA in all culture conditions individually by qRT-PCR. Consistent with the results from miRNA arrays, the induction of miR-141 and miR-429 upon transition from 2-D to rBM 3-D culture were observed only in MCF-7 cells, but not in MDA-MB231 cells (Figure 3, A & B). Moreover, Col-1 abolished the induction of miR-141 and mR-429 in rBM 3-D culture of MCF-7 cells (Figure 3, A & B). On the other hand, the expression of miR-200c was consistently higher in MCF-7 cells than that in MDA-MB231 regardless of the culture conditions (Figure 3C). Consistent with the miRNA array data, let-7c was repressed upon transition from 2-D to rBM 3-D culture only in MCF-7 cells, but not in MDA-MB231 cells (Figure 3D). Col-1 increased the expression of let-7c in rBM 3-D culture of MCF-7 cells (Figure 3D). Overall, these results confirm a correlation between miRNA expression profiles and morphogenesis of breast cancer cells in rBM 3-D culture.

miR-429-mediated attenuation of the invasive stellate morphogenesis of MDA-MB231 cells. To determine the role of miRNAs in morphogenesis of breast cancer cells in rBM 3-D culture, we focused on miR-429 because its expression was high in mass morphogenesis and low in Col-1-disrupted mass morphogenesis of MCF-7 cells, and low in stellate morphogenesis of MDA-MB231 cells (Figure 3B). We chose to determine whether over-expression of miR-429 in MDA-MB231 cells could attenuate stellate morphogenesis and promote mass morphogenesis. We reasoned that knockdown of miR-429 alone in MCF-7 cells may not be sufficient to disrupt mass morphogenesis because other members of miR-200 family, such as miR-141 can compensate a loss of miR-429 in morphogenesis. To this end, we generated MDA-MB231 variants that were transduced with either a backbone vector (MDA-MB231vec) or a miR-429 expressing vector (MDA-MB231miR-429). We compared morphogenesis between MDA-MB231vec and MDA-MB231miR-429 cells in rBM 3-D culture. As expected, MDA-MB231miR-429 exhibited a loss of the invasive stellate morphology and acquisition of mass morphology that resembled MCF-7 cells, whereas MDA-MB231vec retained a stellate morphology that was indistinguishable from the parental MDA-MB231 (Figure 4A). Overexpression of miR-429 was confirmed as MDA-MB231miR-429 exhibited a 62-fold increase in RNA levels of miR-429 over that in MDA-MB231vec (Figure 4B). As a consequence, overexpression of miR-429 repressed its target ZEB2 in MDA-MB231miR-429 to 26% of the control group (Figure 4C) and induced the expression of E-cadherin, a ZEB2 repressed gene, to a 22-fold increase over that in MDA-MB231vec (Figure 4D). These results suggest that miRNAs are crucial regulators of morphogenesis of breast cancer cells in rBM 3-D culture.

Discussion

A recent gene expression profiling of breast cancer cell lines in rBM 3-D culture identifies the gene expression signatures of untranformed and transformed mammary epithelial cell lines displaying distinct morphogenesis (8). Using a similar strategy, we identify the miRNA expression profiles correlating with mass morphology of MCF-7 and stellate morphology of MDA-MB231 cells in rBM 3-D culture. The identified miRNA profiles lend further support to the concept that rBM 3-D culture provides unique and complementary information to morphogenesis and tumorigenesis of mammary epithelial cells (7, 8).

In our comparison of the miRNA profiles between MCF-7 and MDA-MB231 cells, a considerable portion of the differentially expressed miRNAs between MCF-7 and MDA-MB231 cells are common to both 2-D and rBM 3-D cultures (Figure 1, A & B). These miRNAs reflect disparate tumorigenic properties of the two cell lines. For instance, the tumor-promoting miR211~222 cluster is robustly expressed in MDA-MB231 cells and nearly silenced in MCF-7 cells (27). On the other hand, rBM 3-D culture uncovers unique difference between MCF-7 and MDA-MB231 in the expression of miRNAs. This phenomenon appears to result from distinct miRNA response upon transition from 2-D to rBM 3-D culture (Tables 2 and 3). Because rBM 3-D culture promotes differentiation of mammary epithelial cells, a reduced miRNA response of MDA-MB231 relative to MCF-7 implicates that the less aggressive MCF-7 is more responsive to the differentiation-promoting cues derived from rBM 3-D than MDA-MB231 (Table 2 vs. Table 3) (5). This is also congruent to their distinct morphology in rBM 3-D culture. MCF-7 exhibit mass morphology that is characteristic of non-invasive and non-metastatic breast cancer cells, whereas MDA-MB231 cells display stellate morphology that is characteristic of invasive and metastatic breast cancer cells (8).

The MCF-7-specific rBM responsive miRNAs feature increased expression of 3 members of the miR-200 family, miR-200a, miR-141, and miR-429 (Table 2 and Figure 3). Because the miR-200 family is one of the most potent suppressors of EMT, these findings suggest a role of the EMT regulators in morphogenesis of breast cancer cells in rBM 3-D culture. In support of this speculation, robust expression of the miR-200 family members in MCF-7 correlates with the mass morphology that features strong cell-cell adhesion (8). In contrast, the silenced expression of miR-200 family members in MDA-MB231 correlates with the stellate morphology that features disorganized elongated cell clusters with invasive processes in the absence of strong cell-cell adhesion (8). This can be attributed to a loss of ZEB1/2-meidated repression of E-cadherin by robust expression of the miR-200 family in MCF-7 cells, which provides sufficient E-cadherin for strong cell-cell adhesion. These findings also suggest that native BM inhibits EMT and tumor progression via up-regulation of the miR-200 family, and the consequent suppression of the EMT promoter ZEB2. The function of the miR-200 family in morphogenesis is further supported by over-expression of miR-429 in MDA-MB231 cells. Over-expression of miR-429 inhibits the expression of the EMT promoter ZEB2, releases ZEB2-mediated suppression of E-cadherin, and converts the stellate

morphology of MDA-MB231 to a mass-like morphology in rBM 3-D culture (Figure 4). The importance of the rBM responsive miRNAs in morphogenesis is further supported by a comparison of miRNA profiles between rBM 3-D and rBM+Col-1 3-D culture of MCF-7 cells. Col-1 dysregulates the expression of the rBM responsive miRNAs, particularly the miR-200 family, which correlates with disruption of mass morphogenesis of MCF-7 cells (Table 4) (24).

It is noteworthy that the tumor suppressive let-7 miRNA family exhibits a paradoxical decrease in rBM 3-D relative to 2-D culture in MCF-7 and this response is absent in MDA-MB231 (Figure 3B). One plausible explanation of this apparent paradoxical observation is that the expression of let-7 family miRNAs is stimulated in response to tumorigenic cues as a cell defense mechanism and repressed by the rBM derived differentiation-promoting signals. Thus, the decreased expression of the let-7 family implicates that sensing the rBM-derived differentiation promoting cues is intact only in MCF-7 cells, but not in MDA-MB231 cells. A comprehensive functional analysis of the rBM responsive miRNAs in mammary epithelial cells will yield novel insight into how miRNAs regulate mammary epithelial morphogenesis and tumorigenesis.

In summary, the current study provides an initial characterization of miRNA expression that correlates with distinct morphogenesis of breast cancer cell lines in rBM 3-D culture. Our findings strengthen the utility of rBM 3-D culture in elucidating the role of miRNAs in morphogenesis and tumorigenesis of mammary epithelial cells.

List of abbreviations

ECM: extracellular matrix; BM: basement membrane matrix; rBM 3-D: reconstituted basement membrane matrix based three-dimensional organotypic culture; Col-1: type I collagen; EMT: epithelial-mesenchymal transition; miRNA: microRNA; F-actin: filamentous actin; qRT-PCR: quantitative RT-PCR.

Competing interests

The authors declare no competing interests.

Acknowledgements

This work is supported in part by DOD BC085516 awarded to B. Shan. H.T. Nguyen is supported in part by Developmental Funds of the Tulane Cancer Center. geWorkbench is a free open source genomic analysis platform developed at Columbia University with funding from the NIH Roadmap Initiative (1U54CA121852-01A1) and the National Cancer Institute.

References

1. Bissell MJ and Radisky D: Putting tumours in context. Nat Rev Cancer 1: 46-54, 2001.
2. Bhowmick NA, Neilson EG and Moses HL: Stromal fibroblasts in cancer initiation and progression. Nature 432: 332-337, 2004.

3. Weigelt B and Bissell MJ: Unraveling the microenvironmental influences on the normal mammary gland and breast cancer. Semin Cancer Biol 18: 311-321, 2008.
4. Debnath J, Muthuswamy SK and Brugge JS: Morphogenesis and oncogenesis of MCF-10A mammary epithelial acini grown in three-dimensional basement membrane cultures. Methods 30: 256-268, 2003.
5. Hebner C, Weaver VM and Debnath J: Modeling morphogenesis and oncogenesis in three-dimensional breast epithelial cultures. Annu Rev Pathol 3: 313-339, 2008.
6. Lee GY, Kenny PA, Lee EH and Bissell MJ: Three-dimensional culture models of normal and malignant breast epithelial cells. Nat Methods 4: 359-365, 2007.
7. Vargo-Gogola T and Rosen JM: Modelling breast cancer: one size does not fit all. Nat Rev Cancer 7: 659-672, 2007.
8. Kenny PA, Lee GY, Myers CA, et al.: The morphologies of breast cancer cell lines in three-dimensional assays correlate with their profiles of gene expression. Mol Oncol 1: 84-96, 2007.
9. Martin KJ, Patrick DR, Bissell MJ and Fournier MV: Prognostic breast cancer signature identified from 3D culture model accurately predicts clinical outcome across independent datasets. PLoS One 3: e2994, 2008.
10. Trang P, Weidhaas JB and Slack FJ: MicroRNAs as potential cancer therapeutics. Oncogene 27 Suppl 2: S52-57, 2008.
11. Verghese ET, Hanby AM, Speirs V and Hughes TA: Small is beautiful: microRNAs and breast cancer-where are we now? J Pathol 215: 214-221, 2008.
12. Peter ME: Let-7 and miR-200 microRNAs: guardians against pluripotency and cancer progression. Cell Cycle 8: 843-852, 2009.
13. Johnson SM, Grosshans H, Shingara J, et al.: RAS is regulated by the let-7 microRNA family. Cell 120: 635-647, 2005.
14. Sampson VB, Rong NH, Han J, et al.: MicroRNA let-7a down-regulates MYC and reverts MYC-induced growth in Burkitt lymphoma cells. Cancer Res 67: 9762-9770, 2007.
15. Mayr C, Hemann MT and Bartel DP: Disrupting the pairing between let-7 and Hmga2 enhances oncogenic transformation. Science 315: 1576-1579, 2007.
16. Gregory PA, Bert AG, Paterson EL, et al.: The miR-200 family and miR-205 regulate epithelial to mesenchymal transition by targeting ZEB1 and SIP1. Nat Cell Biol 10: 593-601, 2008.
17. Park SM, Gaur AB, Lengyel E and Peter ME: The miR-200 family determines the epithelial phenotype of cancer cells by targeting the E-cadherin repressors ZEB1 and ZEB2. Genes Dev 22: 894-907, 2008.
18. Lin Z, Wang X, Fewell C, Cameron J, Yin Q and Flemington EK: Differential expression of the miR-200 family microRNAs in epithelial and B cells and regulation of Epstein-Barr virus reactivation by the miR-200 family member miR-429. J Virol 84: 7892-7897, 2010.
19. Burow ME, Weldon CB, Tang Y, et al.: Differences in susceptibility to tumor necrosis factor alpha-induced apoptosis among MCF-7 breast cancer cell variants. Cancer Res 58: 4940-4946, 1998.

20. Burow ME, Weldon CB, Chiang TC, et al.: Differences in protein kinase C and estrogen receptor alpha, beta expression and signaling correlate with apoptotic sensitivity of MCF-7 breast cancer cell variants. Int J Oncol 16: 1179-1187, 2000.
21. Shan B, Morris CA, Zhuo Y, Shelby BD, Levy DR and Lasky JA: Activation of proMMP-2 and Src by HHV8 vGPCR in human pulmonary arterial endothelial cells. J Mol Cell Cardiol 42: 517-525, 2007.
22. Paszek MJ, Zahir N, Johnson KR, et al.: Tensional homeostasis and the malignant phenotype. Cancer Cell 8: 241-254, 2005.
23. Shan B, Yao TP, Nguyen HT, et al.: Requirement of HDAC6 for transforming growth factor-beta1-induced epithelial-mesenchymal transition. J Biol Chem 283: 21065-21073, 2008.
24. Li C, Nguyen HT, Zhuang Y, et al.: Post-transcriptional up-regulation of miR-21 by type I collagen. Mol Carcinog 50: 563-570, 2011.
25. Floratos A, Smith K, Ji Z, Watkinson J and Califano A: geWorkbench: an open source platform for integrative genomics. Bioinformatics 26: 1779-1780, 2010.
26. Tusher VG, Tibshirani R and Chu G: Significance analysis of microarrays applied to the ionizing radiation response. Proc Natl Acad Sci U S A 98: 5116-5121, 2001.
27. Rao X, Di Leva G, Li M, et al.: MicroRNA-221/222 confers breast cancer fulvestrant resistance by regulating multiple signaling pathways. Oncogene 30: 1082-1097, 2010.
28. Levental KR, Yu H, Kass L, et al.: Matrix crosslinking forces tumor progression by enhancing integrin signaling. Cell 139: 891-906, 2009.

rBM 3D			
Higher	MCF-7/MB231	Lower	MCF-7/MB231
hsa-miR-141	52.323	hsa-miR-125b	0.002
hsa-miR-429	11.685	hsa-miR-1246	0.026
hsa-miR-345	7.997	hsa-miR-138	0.045
hsa-miR-365	7.376	hsa-let-7c	0.061
hsa-miR-374b	7.102	hsa-miR-181b	0.116
hsa-miR-210	5.325	hsa-let-7g	0.151
hsa-miR-1280	4.545	hsa-miR-30a	0.167
hsa-let-7d*	4.280	hsa-let-7a	0.207
hsa-miR-331-3p	4.207	hsa-let-7b	0.232
hsa-miR-660	3.065	hsa-let-7i	0.237
hsa-miR-197	3.055	hsa-let-7f	0.239
hsa-miR-720	2.936	hsa-let-7e	0.276
hsa-miR-339-3p	2.591	hsa-miR-1275	0.456
hsa-miR-744	2.139	hsa-miR-24	0.466
		hsa-miR-1228	0.472

Table 1. Disparate expression of miRNAs between MCF-7 and MDA-MB231 cells in rBM 3-D culture. Total cell RNA was extracted from MCF-7 and MDA-MB231 cells in rBM 3-D culture. miRNA arrays were carried out and analyzed as described in Methods. A fold change was obtained by setting the values from MDA-MB231 cells to one.

MCF-7			
Higher	rBM 3D/2D	Lower	rBM 3-D/2-D
hsa-miR-149*	7.141	**hsa-miR-605**	**0.057**
hsa-miR-210	**6.881**	**hsa-let-7c**	**0.079**
hsa-miR-762	5.065	**hsa-miR-7**	**0.081**
hsa-miR-548q	**4.732**	hsa-miR-1308	0.126
hsa-miR-141	**4.703**	**hsa-let-7g**	**0.165**
hsa-miR-1469	4.248	**hsa-let-7b**	**0.166**
hsa-miR-331-3p	**4.001**	**hsa-let-7e**	**0.174**
hsa-miR-1260	**3.645**	**hsa-miR-181b**	**0.187**
hsa-miR-200a	**3.375**	**hsa-let-7f**	**0.191**
hsa-miR-1915	3.321	**hsa-let-7a**	**0.209**
hsa-miR-429	**3.148**	**hsa-miR-1246**	**0.262**
hsa-miR-365	**3.135**	**hsa-let-7i**	**0.265**
hsa-miR-1908	2.729	**hsa-miR-1977**	**0.288**
hsa-miR-663	2.701	**hsa-miR-629**	**0.292**
hsa-miR-342-3p	**2.665**	**hsa-miR-1228**	**0.299**
hsa-miR-150*	2.509	**hsa-miR-203**	**0.307**
hsa-miR-1975	2.449	**hsa-let-7d**	**0.327**
hsa-miR-132	**2.445**	**hsa-miR-877**	**0.410**
hsa-miR-425	**2.414**	**hsa-miR-342-5p**	**0.444**
hsa-miR-222	**2.180**	**hsa-miR-1978**	**0.448**
hsa-miR-193a-3p	**2.176**	**hsa-miR-1275**	**0.453**
hsa-miR-193b	**2.093**	**hsa-miR-27b**	**0.459**
hsa-miR-1280	**2.073**	**hsa-miR-940**	**0.481**
hsa-miR-22	**2.007**	**hsa-miR-21**	**0.484**
		hsa-miR-183	**0.495**

Table 2. Disparate expression of miRNAs between 2-D and rBM 3-D cultures of MCF-7 cells. Total cell RNA was extracted from MCF-7 cells in 2-D and rBM 3-D cultures. miRNA arrays were carried out and analyzed as described in Methods. A fold change was obtained by setting the values from 2-D culture of MCF-7 cells to one. Bold font indicated the miRNAs that differed between 2-D and rBM 3-D cultures only in MCF-7 cells, but not in MDA-MB231 cells.

	MDA-MB231		
Higher	rBM 3D/2D	Lower	rBM 3D/2D
hsa-miR-1246	**83.234**	hsa-miR-1308	0.119
hsa-miR-654-5p	**14.009**	**hsa-miR-301a**	**0.177**
hsa-miR-663	8.580	**hsa-miR-381**	**0.203**
hsa-miR-1469	8.121	**hsa-miR-140-3p**	**0.309**
hsa-miR-1915	8.056	**hsa-miR-1280**	**0.407**
hsa-miR-762	7.972	**hsa-miR-18a**	**0.468**
hsa-miR-149*	7.650		
hsa-miR-1826	**6.064**		
hsa-miR-1908	5.710		
hsa-miR-575	**4.718**		
hsa-miR-1231	**4.237**		
hsa-miR-1975	4.107		
hsa-miR-1977	**3.270**		
hsa-miR-1978	**3.219**		
hsa-miR-638	**3.137**		
hsa-miR-1275	**2.671**		
hsa-miR-150*	2.443		
hsa-miR-1974	**2.423**		
hsa-miR-1281	**2.415**		
hsa-miR-193a-5p	**2.371**		
hsa-let-7g	**2.115**		
hsa-miR-27b	**2.071**		

Table 3. Disparate expression of miRNAs between 2-D and rBM 3-D cultures of MDA-MB231 cells. Total cell RNA was extracted from MDA-MB231 cells in 2-D and rBM 3-D cultures. miRNA arrays were carried out and analyzed as described in Methods. A fold change was obtained by setting the values from 2-D culture of MDA-MB231 cells to one. Bold font indicated the miRNAs that differed between 2-D and rBM 3-D cultures only in MDA-MB231 cells, but not in MCF-7 cells.

MCF-7			
Higher	rBM+Col-1/rBM	Lower	rBM+Col-1/rBM
hsa-let-7b	10.896	**hsa-miR-141**	0.086
hsa-let-7e	10.717	hsa-miR-374b	0.105
hsa-miR-605	10.174	**hsa-miR-1280**	0.122
hsa-let-7c	10.142	hsa-miR-27a	0.140
hsa-miR-1246	9.438	hsa-miR-19b	0.149
hsa-miR-1538	7.337	**hsa-miR-200a**	0.152
hsa-let-7a	5.723	hsa-miR-301a	0.192
hsa-let-7f	5.347	hsa-miR-29a	0.195
hsa-miR-1470	5.220	**hsa-miR-429**	0.209
hsa-let-7f-1*	4.636	**hsa-miR-22**	0.221
hsa-miR-943	4.355	hsa-miR-30b	0.222
hsa-miR-1913	3.927	hsa-miR-149*	0.229
hsa-miR-625*	3.764	hsa-miR-720	0.232
hsa-let-7i	3.676	hsa-miR-331-3p	0.250
hsa-miR-519e*	3.516	**hsa-miR-548q**	0.253
hsa-let-7d	3.256	hsa-miR-345	0.270
hsa-miR-342-5p	3.179	hsa-miR-762	0.278
hsa-miR-125a-3p	2.944	hsa-miR-27b	0.323
hsa-let-7g	2.918	hsa-miR-106a	0.342
hsa-miR-629	2.885	hsa-miR-200b	0.354
hsa-miR-877	2.855	hsa-miR-17	0.362
hsa-miR-1249	2.642	**hsa-miR-222**	0.372
hsa-miR-1237	2.533	**hsa-miR-342-3p**	0.376
hsa-miR-21	2.365	hsa-miR-103	0.381
hsa-miR-1308	2.211	hsa-miR-181a	0.383
		hsa-miR-107	0.394
		hsa-miR-455-3p	0.411
		hsa-miR-1301	0.421
		hsa-miR-663	0.442
		hsa-miR-93	0.443
		hsa-miR-23a	0.451
		hsa-miR-425	0.459
		hsa-miR-30d	0.464
		hsa-miR-197	0.466
		hsa-miR-20b	0.482
		hsa-miR-1469	0.496

Table 4. Disparate expression of miRNAs between rBM and rBM+Col-1 3-D cultures of MCF-7 cells. Total cell RNA was extracted from MCF-7 cells rBM and rBM+Col-1 3-D cultures. miRNA arrays were carried out and analyzed as described in Methods. A fold change was obtained by setting the values

from rBM 3-D culture to one. Bold font indicated the miRNAs that commonly differed in comparison between 2-D vs. rBM 3-D and rBM 3-D vs. rBM+Col-1 3-D cultures.

Figure Legends

Figure 1. Distinct miRNA profiles of MCF-7 and MDA-MB231 cells in 2-D and rBM 3-D cultures. A) MCF-7 and MDA-MB231 cells were cultured in rBM 3-D culture for 12 days. Morphogenesis was recorded using an inverse phase contrast microscope. The scale bars are 2.0 mm. B) The cell colonies were visualized using fluorescent staining for F-actin. The images were representatives that were captured at the central planes of cell clusters using a confocal fluorescent microscope at 200x magnification. The images of MDA-MB231 cells were parts of extensively networked cell growth. C) Total cell RNA was extracted from MCF-7 and MDA-MB231 cells in rBM 3-D culture. miRNA expression profiles were compared between the two cell lines using miRNA microarrays. A heatmap of significantly differentially expressed miRNAs and unsupervised hierarchial clustering were generated using geWorkbench suite ($n = 3$, $P < 0.01$, FDR < 0.05). D) Similar to part C except that the miRNA array analysis was carried out on RNA samples collected from 2-D cultures of MCF-7 and MDA-MB231 cells.

Figure 2. Dysregulated expression of miRNAs by Col-1 in rBM 3-D of MCF-7 cells. A) Total cell RNA was extracted from MCF-7 rBM 3-D culture with or without supplementation of Col-1 (2 μg/ml). miRNA expression profiles were compared between the two culture conditions using miRNA microarrays. A heatmap of significantly differentially expressed miRNAs and unsupervised hierarchial clustering were generated using geWorkbench suite ($n = 3$, $P < 0.01$, FDR < 0.05). B) An unsupervised hierarchical clustering analysis was carried out to group and visualize miRNA arrays from MCF-7 cells in 2-D, rBM 3-D, and rBM 3-D + Col-1 cultures according to the expression profiles of miRNAs in each culture condition.

Figure 3. Differential expression of miRNAs among 2-D and rBM 3-D cultures. A) The expression of miR-141 was measured using qRT-PCR in total cell RNA collected from 2-D, rBM 3-D, and rBM 3-D+Col-1 cultures of MCF-7 cells and MDA-MB231 cells. A fold change in miR-141 was obtained by setting the values of miR-141 from MCF-7 cells in 2-D culture to one and normalization to the values of U6. B) Similar to part A except that the expression of miR-429 was compared across the groups. C) Similar to part A except that the expression of miR-200c was compared across the groups. D) Similar to part A except that the expression of let-7c was compared across the groups. The data were presented in averages and standard deviations obtained from three independent experiments. $*$, $**$, and $***$ indicated a P value < 0.05, 0.01, and 0.001, respectively.

Figure 4. Attenuation of the stellate morphology of MDA-MB231 by overexpression of miR-429. A) MDA-MB231vec and MDA-MB231miR-429 cells were cultured in rBM 3-D culture for 12 days. The growth pattern was recorded using an inverse phase contrast microscope. The scale bars are 2.0 mm. B) The expression of miR-429 was measured using qRT-PCR in total cell RNA collected from rBM 3-D cultures of MDA-MB231vec and MDA-MB231miR-429 cells. A fold change in miR-429 was obtained by setting the values of miR-429 from MDA-MB231vec cells to one and normalization to the values of U6. C) Similar to part B except that the mRNA levels of ZEB2 were compared between

MDA-MB231vec and MDA-MB231miR-429 cells. D) Similar to part B except that the mRNA levels of E-cadherin were compared between MDA-MB231vec and MDA-MB231miR-429 cell. The data were presented in average and standard deviations obtained from three independent experiments. $*$, $**$, and $***$ indicated a P value < 0.05, 0.01, and 0.001, respectively.

Figure 1

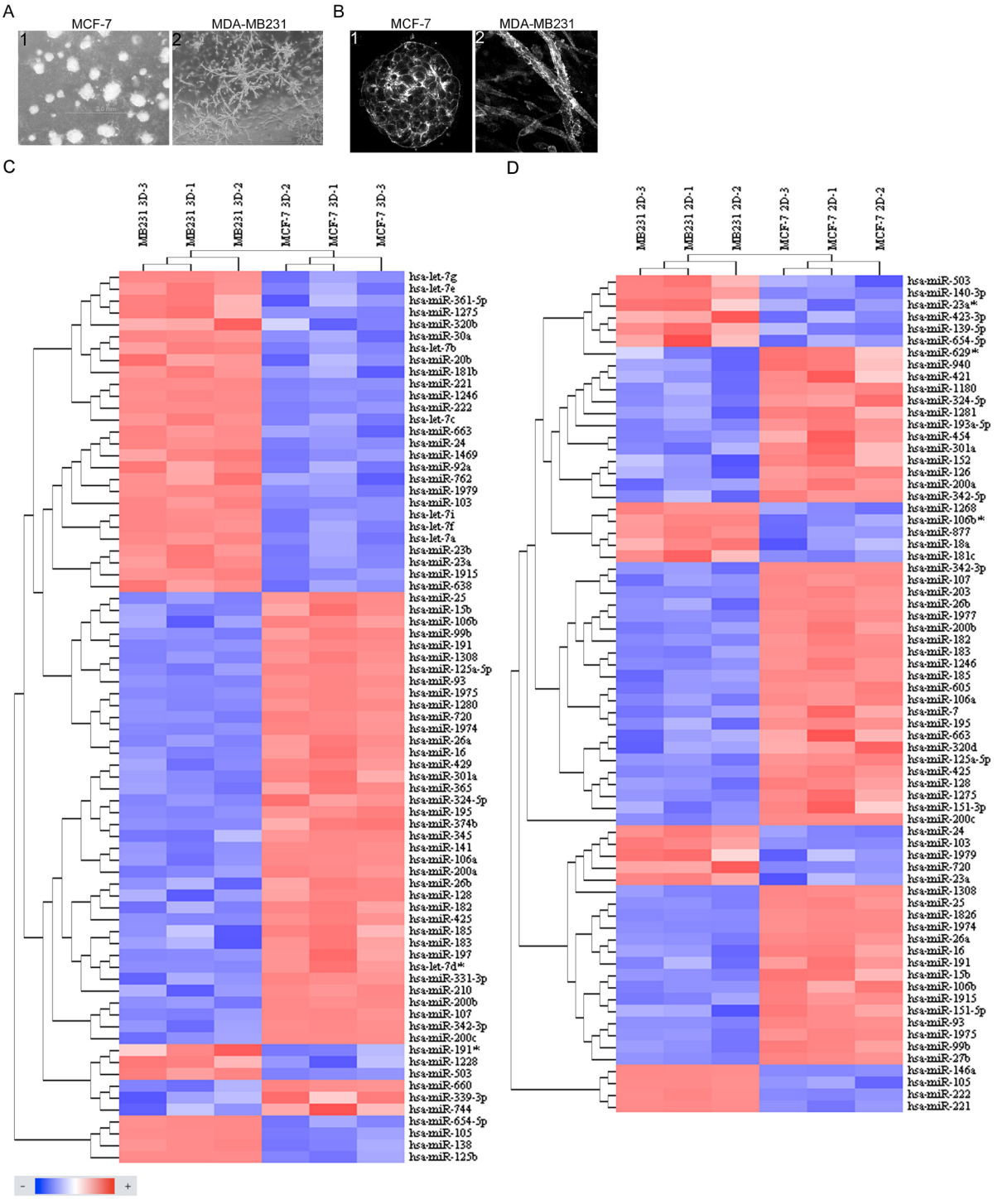
A
MCF-7
MDA-MB231
1
2
B
MCF-7
MDA-MB231
1
2
C
MB231 3D-3
MB231 3D-1
MB231 3D-2
MCF-7 3D-2
MCF-7 3D-1
MCF-7 3D-3
hsa-let-7g
hsa-let-7e
hsa-miR-361-5p
hsa-miR-1275
hsa-miR-320b
hsa-miR-30a
hsa-let-7b
hsa-miR-20b
hsa-miR-181b
hsa-miR-221
hsa-miR-1246
hsa-miR-222
hsa-let-7c
hsa-miR-663
hsa-miR-24
hsa-miR-1469
hsa-miR-92a
hsa-miR-762
hsa-miR-1979
hsa-miR-103
hsa-let-7i
hsa-let-7f
hsa-let-7a
hsa-miR-23b
hsa-miR-23a
hsa-miR-1915
hsa-miR-638
hsa-miR-25
hsa-miR-15b
hsa-miR-106b
hsa-miR-99b
hsa-miR-191
hsa-miR-1308
hsa-miR-125a-5p
hsa-miR-93
hsa-miR-1975
hsa-miR-1280
hsa-miR-720
hsa-miR-1974
hsa-miR-26a
hsa-miR-16
hsa-miR-429
hsa-miR-301a
hsa-miR-365
hsa-miR-324-5p
hsa-miR-195
hsa-miR-374b
hsa-miR-345
hsa-miR-141
hsa-miR-106a
hsa-miR-200a
hsa-miR-26b
hsa-miR-128
hsa-miR-182
hsa-miR-425
hsa-miR-185
hsa-miR-183
hsa-miR-197
hsa-let-7d*
hsa-miR-331-3p
hsa-miR-210
hsa-miR-200b
hsa-miR-107
hsa-miR-342-3p
hsa-miR-200c
hsa-miR-191*
hsa-miR-1228
hsa-miR-503
hsa-miR-660
hsa-miR-339-3p
hsa-miR-744
hsa-miR-654-5p
hsa-miR-105
hsa-miR-138
hsa-miR-125b
-
+
D
MB231 2D-3
MB231 2D-1
MB231 2D-2
MCF-7 2D-3
MCF-7 2D-1
MCF-7 2D-2
hsa-miR-503
hsa-miR-140-3p
hsa-miR-23a*
hsa-miR-423-3p
hsa-miR-139-5p
hsa-miR-654-5p
hsa-miR-629*
hsa-miR-940
hsa-miR-421
hsa-miR-1180
hsa-miR-324-5p
hsa-miR-1281
hsa-miR-193a-5p
hsa-miR-454
hsa-miR-301a
hsa-miR-152
hsa-miR-126
hsa-miR-200a
hsa-miR-342-5p
hsa-miR-1268
hsa-miR-106b*
hsa-miR-877
hsa-miR-18a
hsa-miR-181c
hsa-miR-342-3p
hsa-miR-107
hsa-miR-203
hsa-miR-26b
hsa-miR-1977
hsa-miR-200b
hsa-miR-182
hsa-miR-183
hsa-miR-1246
hsa-miR-185
hsa-miR-605
hsa-miR-106a
hsa-miR-7
hsa-miR-195
hsa-miR-663
hsa-miR-320d
hsa-miR-125a-5p
hsa-miR-425
hsa-miR-128
hsa-miR-1275
hsa-miR-151-3p
hsa-miR-200c
hsa-miR-24
hsa-miR-103
hsa-miR-1979
hsa-miR-720
hsa-miR-23a
hsa-miR-1308
hsa-miR-25
hsa-miR-1826
hsa-miR-1974
hsa-miR-26a
hsa-miR-16
hsa-miR-191
hsa-miR-15b
hsa-miR-106b
hsa-miR-1915
hsa-miR-151-5p
hsa-miR-93
hsa-miR-1975
hsa-miR-99b
hsa-miR-27b
hsa-miR-146a
hsa-miR-105
hsa-miR-222
hsa-miR-221

Figure 2

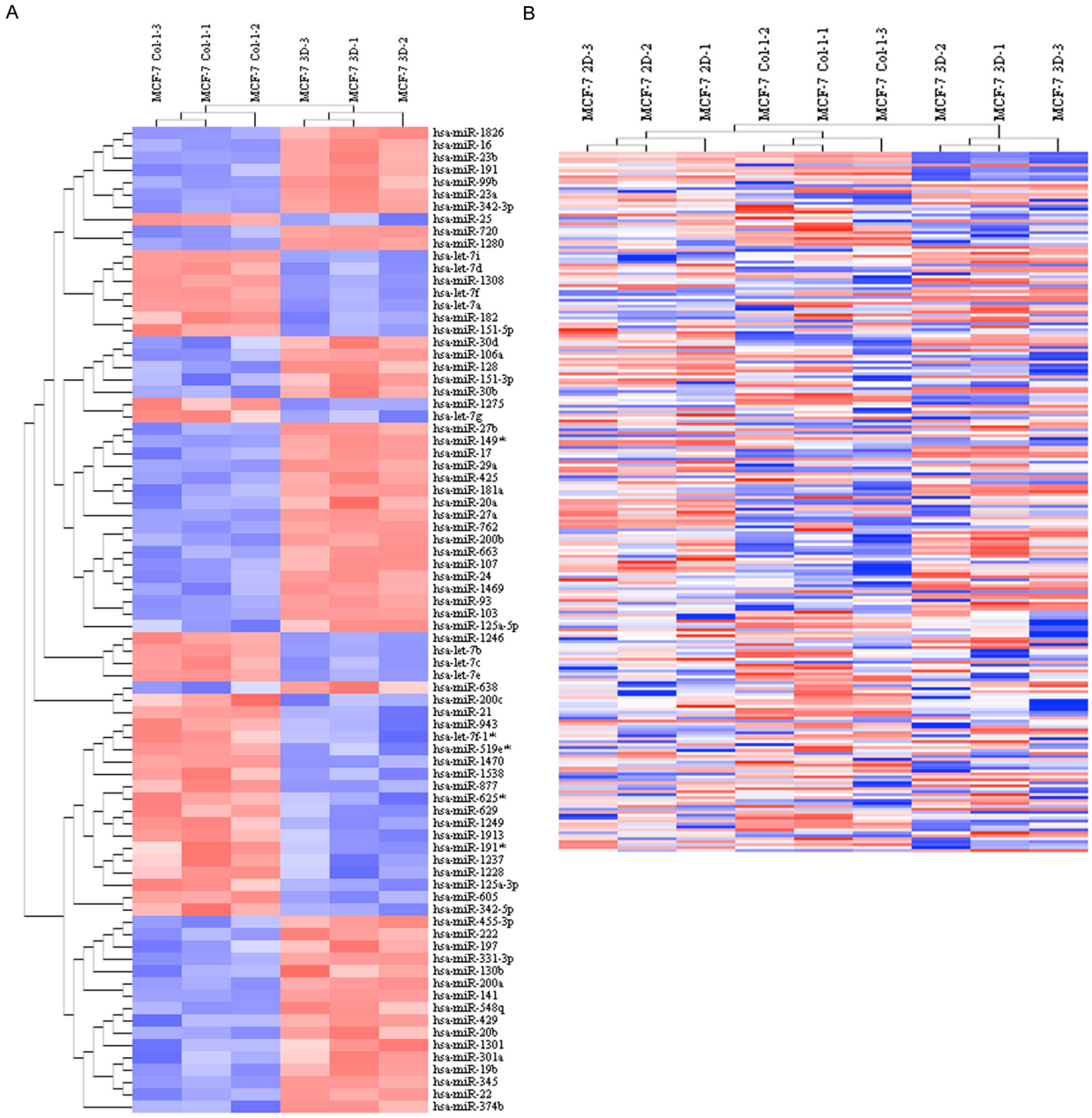
A
MCF-7 Col-1-3
MCF-7 Col-1-1
MCF-7 Col-1-2
MCF-7 3D-3
MCF-7 3D-1
MCF-7 3D-2
hsa-miR-1826
hsa-miR-16
hsa-miR-23b
hsa-miR-191
hsa-miR-99b
hsa-miR-23a
hsa-miR-342-3p
hsa-miR-25
hsa-miR-720
hsa-miR-1280
hsa-let-7i
hsa-let-7d
hsa-miR-1308
hsa-let-7f
hsa-let-7a
hsa-miR-182
hsa-miR-151-5p
hsa-miR-30d
hsa-miR-106a
hsa-miR-128
hsa-miR-151-3p
hsa-miR-30b
hsa-miR-1275
hsa-let-7g
hsa-miR-27b
hsa-miR-149*
hsa-miR-17
hsa-miR-29a
hsa-miR-425
hsa-miR-181a
hsa-miR-20a
hsa-miR-27a
hsa-miR-762
hsa-miR-200b
hsa-miR-663
hsa-miR-107
hsa-miR-24
hsa-miR-1469
hsa-miR-93
hsa-miR-103
hsa-miR-125a-5p
hsa-miR-1246
hsa-let-7b
hsa-let-7c
hsa-let-7e
hsa-miR-638
hsa-miR-200c
hsa-miR-21
hsa-miR-943
hsa-let-7f-1*
hsa-miR-519e*
hsa-miR-1470
hsa-miR-1538
hsa-miR-877
hsa-miR-625*
hsa-miR-629
hsa-miR-1249
hsa-miR-1913
hsa-miR-191*
hsa-miR-1237
hsa-miR-1228
hsa-miR-125a-3p
hsa-miR-605
hsa-miR-342-5p
hsa-miR-455-3p
hsa-miR-222
hsa-miR-197
hsa-miR-331-3p
hsa-miR-130b
hsa-miR-200a
hsa-miR-141
hsa-miR-548q
hsa-miR-429
hsa-miR-20b
hsa-miR-1301
hsa-miR-301a
hsa-miR-19b
hsa-miR-345
hsa-miR-22
hsa-miR-374b
B
MCF-7 2D-3
MCF-7 2D-2
MCF-7 2D-1
MCF-7 Col-1-2
MCF-7 Col-1-1
MCF-7 Col-1-3
MCF-7 3D-2
MCF-7 3D-1
MCF-7 3D-3

Figure 3

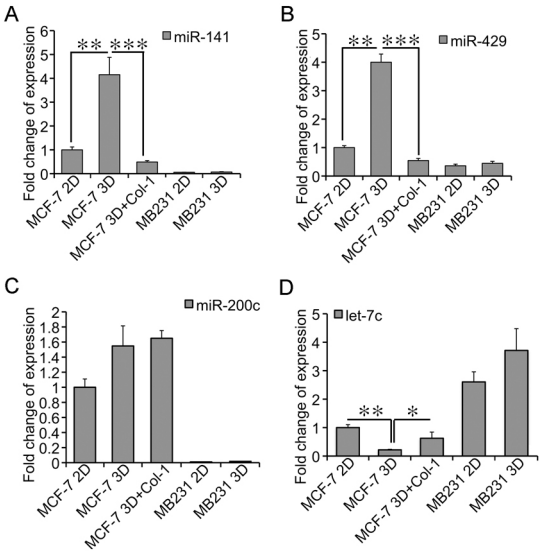
A
miR-141
Fold change of expression
0
1
2
3
4
5
6
** ***
MCF-7 2D
MCF-7 3D
MCF-7 3D+Col-1
MB231 2D
MB231 3D
B
miR-429
Fold change of expression
0
1
2
3
4
5
** ***
MCF-7 2D
MCF-7 3D
MCF-7 3D+Col-1
MB231 2D
MB231 3D
C
miR-200c
Fold change of expression
0
0.2
0.4
0.6
0.8
1
1.2
1.4
1.6
1.8
2
MCF-7 2D
MCF-7 3D
MCF-7 3D+Col-1
MB231 2D
MB231 3D
D
let-7c
Fold change of expression
0
1
2
3
4
5
** *
MCF-7 2D
MCF-7 3D
MCF-7 3D+Col-1
MB231 2D
MB231 3D

Figure 4

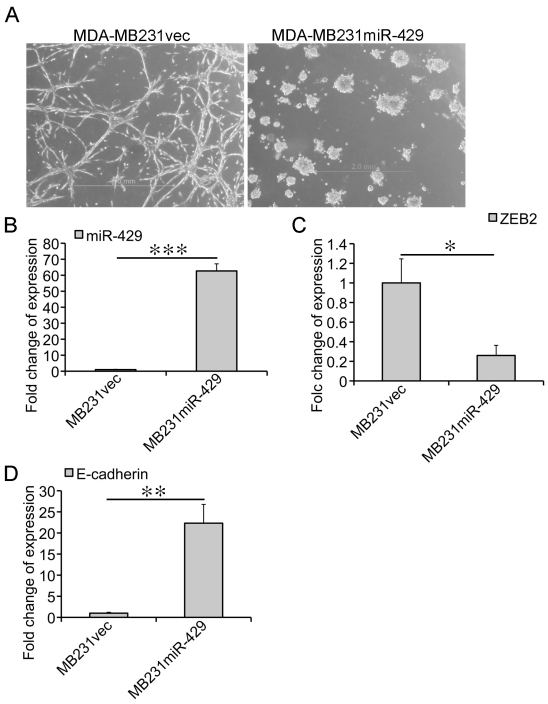
A
MDA-MB231vec
MDA-MB231miR-429
B
miR-429
***
Fold change of expression
80
70
60
50
40
30
20
10
0
MB231vec
MB231miR-429
C
ZEB2
*
Folc change of expression
1.4
1.2
1
0.8
0.6
0.4
0.2
0
MB231vec
MB231miR-429
D
E-cadherin
**
Fold change of expression
30
25
20
15
10
5
0
MB231vec
MB231miR-429